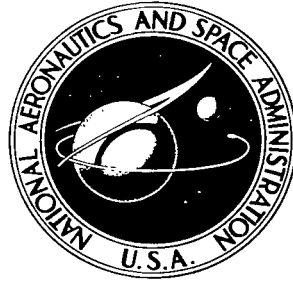NASA TECHNICAL NOTE

NASA TN D-3055

FLIGHT INVESTIGATION OF STABILITY AND CONTROL CHARACTERISTICS OF A 0.18-SCALE MODEL OF A FOUR-DUCT TANDEM V/STOL TRANSPORT

by William A. Newsom, Jr., and Delma C. Freeman, Jr.

Langley Research Center
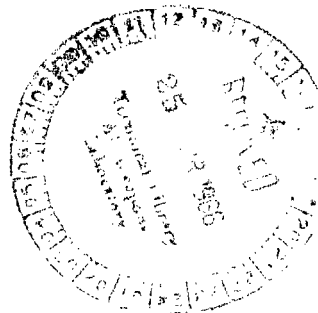Langley Station, Hampton, Va.

FLIGHT INVESTIGATION OF STABILITY AND

CONTROL CHARACTERISTICS OF A 0.18-SCALE MODEL OF A

FOUR-DUCT TANDEM V/STOL TRANSPORT

By William A. Newsom, Jr., and Delma C. Freeman, Jr.

Langley Research Center
Langley Station, Hampton, Va.

Technical Film Supplement L-885 available on request.

FLIGHT INVESTIGATION OF STABILITY AND
CONTROL CHARACTERISTICS OF A 0.18-SCALE MODEL OF A
FOUR-DUCT TANDEM V/STOL TRANSPORT

By William A. Newsom, Jr., and Delma C. Freeman, Jr.
Langley Research Center

SUMMARY

A flight investigation has been made to study the stability and control characteristics of a 0.18-scale model of a four-duct tandem V/STOL transport airplane. The tests included hovering flight in and out of ground effect and level flight and descent conditions in the transition speed range. The model had unstable pitching and rolling oscillations in hovering flight out of ground effect, but it could be controlled and maneuvered easily since the period of these oscillations was long. In hovering flight near the ground, the model experienced large erratic disturbances caused by the recirculation of the ducted-propeller slipstream. The longitudinal stability improved as speed was increased in the transition range and the pitching oscillations were about neutrally stable at the high-speed end of the transition range. Throughout most of the transition speed range, the model had an unstable Dutch roll oscillation and very low directional stability. The Dutch roll instability could be alleviated by the use of artificial damping in yaw. The model also experienced stalling of the upper outside duct surfaces which caused large erratic rolling moments or wing dropping in the landing-approach condition. In all flight regions, the minimum total control powers found to be satisfactory in the model flight tests were approximately equal to or less than the control powers planned for the full-scale airplane.

INTRODUCTION

An investigation to study the low-speed stability and control characteristics of a four-duct tandem V/STOL airplane has been made at the NASA Langley Research Center using a 0.18-scale model.

The investigation included free-flight tests in still air for study of the vertical-take-off-and-landing and hovering-flight conditions, and free-flight tests in the Langley full-scale tunnel for study of slow constant-altitude transitions and simulated descending-flight conditions at transition speeds. The results were mainly qualitative and consisted of pilots' observations and opinions of the behavior of the model.

SYMBOLS

In order to facilitate international usage of data presented, the data are presented in both U.S. Customary Units and in the International System of Units (SI). The equivalent dimensions were determined in each case by using the conversion factors presented in appendix A.

A	total duct exit area, ft^2 (m^2)
$C_{T,s}$	thrust coefficient, $T/q_s A$
c_D	duct chord, ft (m)
D	duct exit diameter, ft (m)
h	height of model fuselage above ground $(\Theta = 0^\circ)$, ft (m)
I_X	moment of inertia about X-body axis, slug-ft^2 (kg-m^2)
I_Y	moment of inertia about Y-body axis, slug-ft^2 (kg-m^2)
I_Z	moment of inertia about Z-body axis, slug-ft^2 (kg-m^2)
i_D	front duct incidence, measured with respect to fuselage, deg
L	lift, lb (N)
L_∞	lift in hover out of ground effect, lb (N)
$M_{X,\phi}$	rolling moment due to roll angle, ft-lb/deg (N-m/deg)
$M_{Y,\theta}$	pitching moment due to fuselage pitch angle, ft-lb/deg (N-m/deg)
M_Z	yawing moment, ft-lb (N-m)
$M_{Z,\infty}$	yawing moment out of ground effect, ft-lb (N-m)
q	free-stream dynamic pressure, lb/ft^2 (N/m^2)
q_s	slipstream dynamic pressure, $q + \dfrac{T}{\pi D^2}$, lb/ft^2 (N/m^2)
S	reference area, 7.26 ft^2 (0.675 m^2)
T	total thrust, lb (N)
V	model velocity, knots
w	weight, lb (N)
X,Y,Z	coordinate axes
α	angle of attack of fuselage, deg

β angle of sideslip, deg

δ_e elevon deflection, deg

θ fuselage pitch angle, deg

ϕ roll angle, deg

APPARATUS AND TESTS

Model

General description.- Photographs of the 0.18-scale model used in the investigation are presented as figure 1. Drawings of the model showing some of the more important dimensions are presented in figure 2. The geometric characteristics of the model are listed in table I and the mass characteristics of the model and the full-scale airplane are compared in table II. It should be noted from table II that the moments of inertia of the model are about 50 percent too high. This situation resulted from the fact that it was not possible to build the gearboxes, shafting, propeller hubs, and ducts nearly light enough to represent their full-scale counterparts; and since these components are major weight items located near the extremities of the model, they caused the moments of inertia to be much too large. The model might, therefore, be regarded as one with properly scaled gross weight, but with excessive moments of inertia; or it might be regarded as being approximately dynamically scaled to represent the aircraft at near empty weight operating at a density ratio of about 0.7, or at a 12 000-foot (3660-meter) altitude. Scaling factors used are given in table III. (See ref. 1.)

The four ducted propellers of the model were interconnected by a system of shafts and gearboxes and were driven by a pneumatic motor. The ducts were pivoted at the 55.1-percent duct-chord station and could be rotated by an electric motor through the complete duct incidence-angle range during flight. The rear ducts, which were mounted at the tip of a fixed wing, had a fixed horizontal stabilizer surface attached to their outboard sides. The front ducts and rear ducts were connected by a simple linkage to give a programed differential duct-angle variation. The programed relationship between front- and rear-duct angle is presented in figure 3. The photograph and sketch in figure 4 show a large-radius fairing that was fitted to the leading edge of the ducts to keep the small-scale ducts from stalling during transition. Results from a number of small-scale duct investigations in the Langley 7- by 10-foot (2.13- by 3.05-meter) tunnel have shown this modification to be necessary in order to simulate the stalling characteristics of the full-scale ducts.

Control system for hovering flight.- In hovering, roll control on the model was provided by differentially acting compressed-air jets exhausting from tubes at the outboard

trailing edge of the ducts. Yaw control was provided by differentially deflecting the elevons mounted in the rear of the ducts. Pitch control was obtained from a jet mounted at the rear of the model. It should be pointed out that on the airplane both pitch and roll control are obtained by differential changes in the total blade pitch angle of the ducted propeller, but on the model, for mechanical reasons, it was not desirable to obtain control from variable propeller-blade pitch. The controls were deflected by flicker-type (full on or off) pneumatic actuators. The actuators were mounted, for trimming, on movable platforms driven by a small electric motor.

Control system for conventional forward flight.- In conventional forward flight where the ducts were near 0° incidence, the model obtained roll and yaw control from the elevons and duct-mounted jets, respectively. The jet reaction control used on the model for pitch control in hovering was also used throughout the investigation from hovering to conventional forward flight. On the airplane, pitch control is obtained from differential deflection of the forward and rear elevons.

Control system for transition flight.- In the transition range the duct-mounted jets and the elevons interchange their function as the duct incidence angle changes. On the full-scale airplane, a control mixing device is used to give the desired response to the pilot's control movements. No such mechanical mixer was used in the model investigation, but the model pilots were able to use various combinations and amounts of the lateral-directional controls by electrical switching of the flicker mechanisms and by ground adjustment of the amount of control given by the flicker mechanism. The control moments used during the different flight conditions are presented subsequently.

Test Techniques

The basic test setup used in the present tests was essentially the same as that used for all flight tests in the Langley full-scale tunnel and is illustrated in figure 5. An additional operator (not shown in fig. 5) was located near the pitch pilot to control the duct incidence in some of the tests. The power for the duct tilt motor, the control trim motors, and the electric-control solenoids was supplied through wires; and the air for the pneumatic motors, the jet-reaction controls, and the control actuators was supplied through flexible plastic tubes. These wires and tubes were suspended from the top of the tunnel and were taped to a safety cable (1/16-inch (1.6-mm) braided aircraft cable) from a point about 15 feet (4.57 meters) above the model down to the model itself. The safety cable, which was attached to the fuselage near the model center of gravity, was used to prevent crashes in the event of a power or control failure or in the event that the pilots lost control of the model. Separate pilots are used to control the model in pitch, roll, and yaw. The reasons for using this model flight technique in which the piloting duties are divided in preference to the conventional single-pilot technique are explained in

4

detail in reference 2. In forward (and descending) flight, sometimes only two pilots were were used - one pilot controlled both roll and yaw.

Tests to study the level-flight transition characteristics of a model can be made in the Langley full-scale tunnel either by continually increasing or decreasing the tunnel airspeed until the transition is completed or by holding the tunnel airspeed constant at intermediate speeds for more careful study of any stability and control characteristics or problems that may be encountered.

It has been found in previous work with some V/STOL aircraft (see ref. 3) that one of the most critical flight conditions is the partially transitioned steady-state descent condition which will probably be used for most landing approaches. In order that this condition might be studied in the present investigation, the free-flight testing technique in the Langley full-scale tunnel has been extended, as described in reference 4, to permit tests simulating the steady-state descent condition in the horizontal airstream of the tunnel.

For hovering tests, a test setup similar to that shown in figure 5 is made in a special hovering test area located in a large enclosure where the pilots can be stationed closer to the model than is possible in the tunnel test section. It has been found very desirable, particularly during tests in which the model is flown very close to the ground, for the pilots to be near the model so that they can observe more readily and correct for slight changes in model attitude and altitude more quickly.

Tests

The free-flight investigation included tests at three different flight conditions: (1) hovering, both in and out of ground effect, (2) steady-level forward flight, with the fuselage at several different angles of attack, over the whole transition range from hovering to near cruise, and (3) simulated descent flight at $i_D = 20^O$, 30°, 40°, and 50° for descent angles of 0°, 5°, 7°, 10°, 13°, and 15°. The stability, controllability, and the general flight behavior were determined qualitatively from the pilots' observations; and motion-picture records of the flight tests were made as an aid in the pilots' evaluation and to supply some quantitative data on the model motions. Most of the flight tests were made without artificial stabilization, but for a few tests, artificial rate damping was installed about the yaw axis.

The basic stability of the model was studied, in each flight condition, by having two of the pilots control the model as steadily as possible (after a trimmed condition had been established) while the third pilot made the required tests to determine the stability of a particular phase of the model motion. In that manner, for example, the control-fixed pitching or rolling motions of the model were determined. The controllability was determined in the same manner with each pilot in turn varying his control power to

determine the amount of control required for steady flying and for performing various maneuvers. The basic stability or control characteristics of a model do not, however, give the complete picture of the model flight characteristics; therefore, the model pilots also assessed its general flight behavior, including the effects of such factors as stalling.

A few force tests were made, in addition to the free-flight tests, to help document some of the aerodynamic and stability and control characteristics of the model. These tests were quite limited, however, since an extensive force-test investigation of the configuration had been conducted at approximately the same model scale. (See ref. 5.)

RESULTS AND DISCUSSION

A motion-picture film supplement (L-885) to this report has been prepared and is available on loan. A request card form and a description of the film are bound at the back of this paper.

In reviewing the results of the flight tests, it should be remembered that, as shown in table II, the scaled-up moments of inertia of the test model were high in comparison with the full-scale values. The high moment-of-inertia characteristics of the model could have affected the detailed results of this investigation; for example, they could cause very slight changes in the period of the hovering oscillations or slight changes in the damping of the lateral oscillatory motions in forward flight. It is believed, however, that the conclusions reached from the model flight tests are valid because any effect of the high moments of inertia was negligible since the periods of the motions experienced with this model were relatively long.

Hovering Out of Ground Effect

The flight tests, in still air out of ground effect, were conducted to determine the basic stability in hovering flight. These tests showed that the model had unstable control-fixed oscillations in pitch and roll and was neutrally stable in yaw. Examples of the motions encountered in pitch and roll are shown by the time histories presented in figures 6 and 7. These time histories were obtained from motion-picture records of the model flights. The period of the pitching oscillation was about 3.4 seconds and the period of the rolling oscillation was about 3.0 seconds. These values scale up to about 8 and 7 seconds, respectively, for the full-scale airplane.

In spite of the fact that the model had these unstable control-fixed pitching and rolling oscillations, the pilots felt that the general flight behavior of the model was fairly good. They could control these oscillations easily, and the model could be flown smoothly and could be maneuvered readily from one position to another. One reason that the model was easy to control in spite of the unstable oscillations was that the periods of

the oscillation were fairly long and thus the pilot was not conscious of its presence in normal flying. Another reason that the model was easy to control was that the motions were relatively slow in starting and were not excited by outside effects such as gust disturbances at this altitude and under these test conditions.

One factor which affected the hovering flight behavior of the model was a cross coupling of the yaw control with roll. This cross coupling resulted from a combination of the resultant slipstream rotation, which is in a different direction on each side of the configuration, in conjunction with deflection of the elevons for yaw control. It was found in force tests that the movement of the elevons in the ducts for yaw control caused an adverse rolling moment equal to a minimum of 15 percent of the yaw control moment obtained. This interaction is a function of the propeller parameters and operating conditions. It is not possible to duplicate all of these conditions exactly with the model, but since this interaction was obviously important, the model characteristics, such as propeller torque and direction of rotation, were set up to duplicate the full-scale slipstream rotation as closely as possible. Another factor that could affect the amount of interaction would be any stalling that might occur on the elevons as a result of slipstream rotation and large elevon deflections. In any event, the cross coupling experienced on the model was noticeable to the pilots during the hovering flight tests but did not materially affect their opinion of the model's flight behavior because of the small amount of yaw control required for the steady flying conditions tested. This characteristic might be more objectionable, however, in conditions requiring extensive use of yaw control.

In the flight tests to determine how much control power was required for steady flight and for performing various maneuvers, the pitch pilot found that slightly more control acceleration was required for satisfactory controllability than is provided in the full-scale airplane. The full-scale airplane is designed to provide for the following control power in excess of that needed for trim in a 35-knot wind: accelerations of 0.60 radian/sec^2 in pitch, 1.00 radian/sec^2 in roll, and 0.56 radian/sec^2 in yaw. Actually, the model pilots found that about 110 percent of the scaled-down value in pitch, 80 percent of the scaled-down value in roll, and 30 percent of the scaled-down value in yaw was needed for performing the test maneuvers required of the model. It has been found, as pointed out in reference 2, that model flight-test results generally correlate well with full-scale flight-test results on the control power required in pitch and roll, but that the yaw-control requirements have not shown correlation with full-scale experience. The yaw-control task in model flying is mainly one of simple alinement under steady flying conditions and does not involve gusts, operation in cross winds, maneuvering in yaw, or other disturbances and trim requirements found in full-scale tests which might require larger amounts of control power.

Hovering in Ground Effect

The variation of static stability with height above the ground, as measured in force tests, is shown in figure 8. These data show that the model had a small amount of static stability in pitch for nose-down fuselage angles, but at nose-up fuselage angles the configuration was stable only very near the ground. The data also show that the model was statically unstable in roll. The main factor affecting these results is the slipstream effect on the difference in fuselage bottom-area distribution forward and rearward of the center of gravity and the large wing area at the rear of the model. Reference 6 discusses slipstream flow effects on a tilt-duct configuration for bank angles in ground effect.

In the flight tests, the model experienced very strong erratic disturbances when hovering near the ground; these disturbances made the model very difficult to control. In fact, the roll pilot could not obtain a flight condition steady enough in ground effect to allow the other pilots and the power operator to obtain an adequate evaluation of the flight characteristics. During short periods of relatively steady flights, however, the pitch pilot did detect a slight improvement in the pitch stability.

The static instability in roll could have contributed to the roll pilot's problems. It is believed, however, that the major difficulty in the model's flight behavior in ground effect was caused by the dynamic effect of the random recirculation of the fan slipstreams. In addition to the normal ground effect of the slipstreams meeting under the model and pushing up on the fuselage, tandem configurations such as this model have another strong source for disturbances. Near the ground, the fan slipstreams meet and form a strong upward flow between the fore and aft ducts that tends to flow erratically into one fan or the other. These flows, along with the flow under the fuselage are not stable and are further influenced by the model motions and by the deflection of the elevons in the fan slipstreams for yaw control.

As previously mentioned, flight investigation of the effect of ground proximity on lift and yaw control was severely restricted by the difficulty with the roll behavior. However, force-test data were obtained and are presented in figures 9 and 10. The data of figure 9 show the variation of lift at constant propeller speed with height above the ground. The data show a 20-percent increase in model lift at the height corresponding to wheel touchdown on the full-scale airplane with the shock struts fully extended. Analysis of the data of reference 7 indicates that practically all of the 20-percent increase in lift was caused by an upload on the bottom of the fuselage. The source of this upload is discussed in more detail in references 3, 7, and 8.

The data of figure 10 show a decrease of about 40 percent in yaw-control moment produced by the elevons near the ground but the pilot believed that there was still satisfactory control available for model test purposes. This decrease in elevon effectiveness

8

is partially explained by the decrease in the fan thrust required in ground effect since the data of figure 10 were obtained for the lift required for steady flight at each height.

The generally poor flight behavior of the model near the ground does not necessarily mean that the full-scale aircraft could not be flown under good flight conditions. Past flight experience with full-scale V/STOL aircraft has indicated, however, that disturbances on models much less severe than those experienced on this model were objectionable to the pilot flying the full-scale aircraft. The flight behavior of this model would therefore seem to indicate that artificial stabilization would be required to obtain satisfactory flight behavior in ground effect.

Level Flight in Transition

Longitudinal stability.- The basic stability of the model throughout the transition flight range was determined during constant-airspeed flight tests with the model trimmed for flight at various angles of attack. Examples of the type of motions experienced are shown in figure 11 which presents time histories of the control-fixed pitching motions for front-duct incidence angles representing five different airspeeds at $\alpha = 0^O$. The relation between model velocity and front-duct incidence angle is shown in figure 12. The curves of figure 11 show that, as noted previously, the control-fixed motion in hovering was an unstable oscillation. At a front-duct incidence of 72° the instability of the motion had decreased and the period was about double the period of the hovering oscillation. The unstable motion at this high duct-incidence angle was not very noticeable to the pilot when he was flying the model in the normal manner. When the period of the longitudinal motion is as long as 5 or 6 seconds for a model the size of the present one, it has been found that, without looking carefully for the oscillation at constant forward speed, the pilot would not ordinarily distinguish it from the normal gust, or other disturbances that the model experiences in flight tests. At the lowest duct-incidence angle shown $\left(i_D = 30^O\right)$, the period of the motion was very long and the motion appeared almost as an out-of-trim flight condition. This progressive change from a longitudinally unstable to an apparently stable flight condition as the transition progresses from hovering to forward flight is typical of other V/STOL configurations such as that of reference 4.

Lateral stability.- In the transition range of flight, the model exhibited Dutch roll oscillations that were unstable in the low-speed range and were still very lightly damped to quite high speeds corresponding to a duct angle of about 20°. The behavior of the model was considered dangerous and likely to cause damage to the model at this condition because of the higher airspeeds involved; therefore, tests of the basic configuration were not made at lower duct angles. Three principal factors contributed to this Dutch roll tendency: The model had about neutral directional stability in this flight range; it

had large effective dihedral, and the principal axis was inclined downward about 8°. It was quite difficult to fly the model through the transition range with the fuselage level. It was found that a nose-up attitude of about 5° helped considerably to damp the oscillations but the flight tests were still terminated at a duct angle of about 20°.

As a first effort to improve the lateral-directional flight characteristics, the vertical-tail area was increased to improve the directional stability of the configuration. Figure 13 presents the results of force tests of the model for $i_D = 50^O$, 40°, 30°, and 20° with vertical tail off, tail on, and with 31.2-percent larger vertical-tail area. The increase in tail area was made by adding an extension to the trailing edge of the basic tail as shown in figure 2. The data of figure 13 show that the increased tail area made very little difference in the directional characteristics until speeds, or dynamic pressures, corresponding to a duct angle of 30° or less were reached. Although the data showed a stable variation of yawing moment with angle of sideslip at higher duct angles, the forces developed at the low dynamic pressures resulted in very low stability; the behavior of the model observed in flight was typical of that of a configuration having neutral directional stability. In any event, the increased tail area did not have a significant effect on the lateral-directional oscillations.

A second device tried in an effort to improve the lateral-directional flight characteristics was a yaw rate damper. This increased directional damping essentially fixed the Dutch roll problem and permitted flight tests to be made over the entire transition range of flight.

The model had another problem or characteristic which contributed to the poor lateral-directional behavior. It was found that the model was experiencing stall on the upper outside surfaces of the ducts over a fairly large range of level flight conditions from about 60° to 20° duct angle. At the higher duct angles in this range (about 60° to 30°), the resultant disturbances to the model were small, because of the low airspeeds, and were experienced mostly in yaw. At the lower duct angles (about 30° to 20°), the dynamic input of the disturbances due to stalling was larger because of the higher dynamic pressure, and mostly about the roll axis because of the low duct angles. In these cases, the model experienced erratic and very objectionable rolling motions or wing dropping.

A series of tuft studies was made with the model mounted on a strut in the tunnel to study the stalling problem. It was found that, in some flight conditions, there was intermittent, erratic stalling of the upper surfaces of the ducts, and that over an angle-of-attack range, these duct upper surfaces did not stall symmetrically. The results of a typical tuft test are shown in figure 14. The figure shows a series of tuft photographs which illustrates the upper-surface stall experienced on the model at a duct incidence

angle of 20° as the fuselage angle of attack is varied from -1^O to $+6^O$. First, figure 14(a) shows that all the duct upper surfaces are unstalled at $\alpha = -1^O$. Next, figure 14(b) indicates that at $\alpha = 1^O$, the right front duct begins to stall across the top. Figure 14(c) shows that both front ducts are stalling at $\alpha = 2^O$. Due to the duct programing, the rear ducts were at an incidence angle about 4° less than that of the front ducts so that the right-rear duct stalled at $\alpha = 5^O$ (fig. 14(d)) and the left-rear duct stalled at $\alpha = 6^O$ (fig. 14(e)). It was found in these tests that there was an intermittent stall condition on each duct surface for an incidence angle at least 1^O less than the stall angle of attack so that at a given test condition there might be an unstalled duct, an intermittently stalling duct, and a stalled duct on the model all at the same time. These tests also showed that sideslip angle affected the upper-surface duct stalling by moving the stalled area towards the downstream side of the ducts.

In an attempt to delay the stall of the duct upper surfaces and have it occur outside the normal range of operating conditions, various types of vortex generators were investigated. As shown in figure 15, trip wire, wedge, and vane vortex generators were tested but none had any noticeable effect on the duct stalling. A set of leading-edge slats were fitted to the model as shown in figure 16. The slats were positioned, as shown in figure 16(a) and covered an arc of about 90°. Tuft tests, made with the slats mounted as shown, indicated that the slats delayed the stall to a fuselage angle of attack of at least 10° for all duct incidence angles, and to as much as 20° angle of attack at low duct-incidence angles where the disturbances due to the stalling had been the most objectionable.

With the slats mounted on the ducts, the model was again tested in flight throughout the transition range. As expected, the model, with slats, did not experience the erratic and objectionable rolling motions or wing dropping. These tests afforded proof that it was the erratic upper-surface stall that was causing the wing dropping and generally erratic lateral behavior of the basic model. It should be realized that this duct stalling might be subject to scale effect, and this point is discussed in some detail in subsequent discussion of the descent tests.

It should be noted here that although the slats solved the wing dropping, the model still had the Dutch roll tendency and artificial damping in yaw was still required for satisfactory flight characteristics. However, by flying at an angle of attack of 5° to reduce the Dutch roll problem, tests could be made without the rate damper at a speed much higher than had been considered safe before the slats were installed. Flights were made up to and including a model velocity of approximately 54.5 knots (129 knots, full scale). It was found that, with the increased tail area, there was noticeable improvement in the directional stability of the model from about $V = 44.5$ knots up to about $V = 49.2$ knots. Above $V = 49.2$ knots, the directional stability was very good and the rolling-moment characteristics which had been slowly improving also were quite satisfactory.

Descending Flight in Transition

Normally, a small-scale duct surface would be expected to stall at a lower angle of attack than the full-scale duct surface. For this reason, the duct upper-surface stalling experienced in this small-scale investigation may not be experienced on the full-scale aircraft at the same flight conditions. Figure 17 shows a comparison of the expected stall boundaries for the model and the full-scale aircraft by means of a plot of thrust coefficient $C_{T,s}$ against duct angle. The expected full-scale boundary was obtained from unpublished data for a single large-scale duct of similar configuration. Figure 17 shows that for a given thrust coefficient, the small-scale duct stalls at duct incidence angles from 5° to 8° lower than those for the full-scale duct.

In figure 18, the stall boundaries of figure 17 are repeated and lines representing level flight, 500 ft/min (2.54 m/sec), and 1000 ft/min (5.08 m/sec) rates of descent (full scale) have been added to better show the significance of the difference between the stalling characteristics of the model and full-scale aircraft. The approximate full-scale velocities are also shown on this plot. The data of figure 18 indicate that, although the model experienced stall in level flight over a large range of duct angles, the full-scale aircraft would not be expected to experience these disturbances in level flight - at least not for the steady test conditions in the absence of gusts or other dynamic disturbances which these data represent. However, figure 18 does show that the aircraft could experience stall in a lower powered descending or deceleration flight condition in a speed range where the aircraft would be expected to be making steep approaches to a landing. These possible disturbances from intermittent stalling, along with the fairly low directional stability in the approach speed range combined with the lightly damped to unstable Dutch roll tendency would probably result in very poor flying qualities for the basic aircraft without stability augmentation, and pilot difficulty would be further increased under instrument flight conditions.

A few flight tests were made in the present investigation in simulated descent flight over a range of duct incidence angles from 50° to 20° for descent angles from 0° to 15°. However, the results were not directly applicable because of the difference in stalling characteristics shown previously. The basic model, without the slats, stalled even in level flight but with the slats installed, the duct upper surfaces did not stall for any of the conditions tested.

In the tests of the basic model without slats, the pilots did notice a definite improvement in the flight behavior of the model at modest descent angles as compared with level flight over most of the speed range. The flights were smoother and the roll pilot commented that there was a marked improvement in the roll damping characteristics of the model after a disturbance. Actually, tuft studies showed that, at these flight conditions, the duct upper surfaces were completely stalled. These flight-test results indicated

12

again, therefore, that it was the intermittent stalling of the duct upper surfaces that was causing the wing dropping and the worst of the poor flight behavior of the basic model in level flight. Although the free-flight model tests did not predict the conditions at which upper-surface stall would occur, they did indicate the type of motion that would result.

Evaluation of Control Power Required

Longitudinal control.- As mentioned previously, the pitch jet was used throughout the flight range to provide the longitudinal control required for maneuvering. Figure 19 shows the longitudinal control power, in excess of that required for trim, planned for the airplane compared with the pitch-jet longitudinal control power (scaled up to full-scale values) required on the model. The longitudinal control used on the model was found to be adequate for any of the test conditions including some rather abrupt maneuvering in both level and descending flight as well as in hovering flight.

Lateral control.- As pointed out previously, in the transition-flight mode, the full-scale aircraft has a control mixing device which provides, at each angle of duct incidence, a predetermined combination of propeller pitch and elevon deflection in response to a roll or yaw control from the pilot. The controls were not mechanically phased on the model but the roll and yaw pilots could command preselected amounts and combinations of control moment during the transition in order to study the control requirements. Figure 20 shows the planned control powers for full lateral stick control and full rudder pedal control on the full-scale aircraft, in terms of angular accelerations, along with the control powers found to be required during the present model tests scaled up to full-scale values. In all cases the maximum control powers found desirable by the model pilots were less than those planned for the full-scale aircraft.

SUMMARY OF RESULTS

The results of the flight tests of the 0.18-scale model of a four-duct tandem V/STOL transport may be summarized as follows:

1. Hovering-flight tests out of ground effect showed that basic controls-fixed motions of the model consisted of unstable oscillations in pitch and roll and that the model was neutrally stable in yaw. The unstable oscillations were of relatively long period, however, and were very easy for the pilot to control.

2. Hovering-flight tests in ground effect showed that the model experienced significant erratic disturbances, particularly in roll, from recirculation of the ducted-propeller slipstream, which made the model very difficult to control.

3. In the transition speed range, no trouble was experienced with the longitudinal stability, but the Dutch roll oscillation was either unstable or neutrally stable over most of the transition speed range at 0° angle of attack. This Dutch roll instability resulted to a considerable extent from the fact that the model had neutral or low directional stability over the whole transition flight range. The Dutch roll instability could be alleviated by the use of a yaw-rate-damper stability-augmentation device. Further lateral-directional difficulties resulted from the fact that the model experienced intermittent stalling of the upper surfaces of the ducts over much of the transition range. In particular, this duct stalling resulted in large erratic rolling moments, or wing dropping, at duct angles of attack of about 20° to 30°.

4. In all flight regions, the minimum total control powers found to be satisfactory in the model flight tests were about equal to or less than the control powers planned for the full-scale airplane.

Langley Research Center,
    National Aeronautics and Space Administration,
        Langley Station, Hampton, Va., September 22, 1965.

APPENDIX A

CONVERSION FACTORS - U.S. CUSTOMARY UNITS TO SI UNITS

Physical quantity	U.S. Customary Unit	Conversion factor (*)	SI Unit
Force	lbf	4.4482	newtons (N)
Length . . . . {	in.	0.0254	meters (m)
	ft	0.3048	meters (m)
Moment	ft-lb	1.3558	newton-meters (N-m)
Moment of inertia . . .	slug-ft^2	1.3558	kilogram-meter^2 (kg-m^2)
Pressure	lb/ft^2	47.8802	newtons/meter^2 (N/m^2)
Area . . . . {	in^2	6.4516	centimeters^2 (cm^2)
	ft^2	0.0929	meters^2 (m^2)
Velocity	ft/min	0.00508	meters/second (m/s)

*Multiply value given in U.S. Customary Unit by conversion factor to obtain equivalent value in SI Unit.

Prefix	Multiple
centi (c)	10^{-2}
milli (m)	10^{-3}

REFERENCES

1. Shortal, Joseph A.; and Osterhout, Clayton J.: Preliminary Stability and Control Tests in the NACA Free-Flight Wind Tunnel and Correlation With Full-Scale Flight Tests. NACA TN 810, 1941.

2. Parlett, Lysle P.; and Kirby, Robert H.: Test Techniques Used by NASA for Investigating Dynamic Stability Characteristics of V/STOL Models. J. Aircraft, vol. 1, no. 5, Sept.-Oct. 1964, pp. 260-266.

3. McKinney, M. O.; Kirby, R. H.; and Newsom, W. A.: Aerodynamic Factors To Be Considered in the Design of Tilt-Wing V/STOL Airplanes. Vertical Take-Off and Landing (VTOL) Aircraft. Ann. N.Y. Acad. Sci., vol. 107, art. 1, Mar. 25, 1963, pp. 221-248.

4. Newsom, William A., Jr.; and Kirby, Robert H.: Flight Investigation of Stability and Control Characteristics of a 1/9-Scale Model of a Four-Propeller Tilt-Wing V/STOL Transport. NASA TN D-2443, 1964.

5. Spreemann, Kenneth P.: Wind-Tunnel Investigation of Longitudinal Aerodynamic Characteristics of a Powered Four-Duct-Propeller VTOL Model in Transition. NASA TN D-3192, 1966.

6. Kelley, Henry L.: Transition and Hovering Flight Characteristics of a Tilt-Duct VTOL Research Aircraft. NASA TN D-1491, 1962.

7. Newsom, William A., Jr.: Effect of Ground Proximity on the Aerodynamic Characteristics of a Four-Engine Vertical-Take-Off-and-Landing Transport-Airplane Model With Tilting Wing and Propellers. NACA TN 4124, 1957.

8. Schade, Robert O.: Ground Interference Effects. NASA TN D-727, 1961.

TABLE I.- GEOMETRIC CHARACTERISTICS OF MODEL

Fuselage:

Length . . . . 6.70 ft (204.0 cm)

Cross-sectional area, maximum . . . . 1.01 ft^2 (940.0 cm^2)

Height, maximum . . . . 1.44 ft (43.9 cm)

Width, maximum . . . . 1.10 ft (33.5 cm)

Wing:

Aerodynamic reference area . . . . 7.26 ft^2 (6750.0 cm^2)

Aerodynamic reference chord . . . . 1.26 ft (38.4 cm)

Aerodynamic reference span . . . . 6.89 ft (210 cm)

Chord . . . . 1.50 ft (45.7 cm)

Airfoil section . . . . NACA 2419

Sweep angle of 0.25 chord . . . . 0°

Distance from 0.25 chord to center of gravity . . . . 1.79 ft (54.6 cm)

Horizontal stabilizers outboard of rear ducts (two panels):

Area . . . . 0.67 ft^2 (62.3 cm^2)

Mean aerodynamic chord . . . . 0.85 ft (26.0 cm)

Sweep angle of 0.25 chord . . . . 9°

Airfoil section . . . . NACA 0015

Distance from 0.25 stabilizer M.A.C. to
center of gravity . . . . 1.72 ft (52.4 cm)

TABLE I.- GEOMETRIC CHARACTERISTICS OF MODEL - Concluded

	Basic	Large
Vertical tail:		
Area	2.22 ft^2 (2063.0 cm^2)	2.92 ft^2 (2717.0 cm^2)
Span	2.07 ft (63.1 cm)	2.07 ft (63.1 cm)
Mean aerodynamic chord . . .	1.09 ft (33.2 cm)	1.43 ft (43.6 cm)
Aspect ratio	1.92	1.47
Root chord	1.30 ft (39.6 cm)	1.65 ft (50.3 cm)
Tip chord	0.84 ft (25.6 cm)	1.17 ft (35.7 cm)
Taper ratio	0.64	0.71
Sweep angle of 0.25 chord . . .	20°	
Distance from 0.25 tail M.A.C. to center of gravity	2.57 ft (78.3 cm)	2.65 ft (80.7 cm)
Airfoil section -		
Tip	Modified NACA 0011	Modified NACA 0011
Root	Modified NACA 0017	Modified NACA 0017

	Forward	Aft
Elevons (each):		
Area	0.82 ft^2 (76.2 cm^2)	1.06 ft^2 (98.6 cm^2)
Span	1.40 ft (42.6 cm)	1.40 ft (42.6 cm)
Mean aerodynamic chord . . .	0.65 ft (19.8 cm)	0.79 ft (24.1 cm)
Aspect ratio	2.38	1.84
Taper ratio	1.00	1.00
Sweep angle of 0.25 chord . . .	0°	0°
Airfoil section	Modified NACA 0014	Modified NACA 0009
Duct:		
Exit diameter	1.40 ft (42.7 cm)	1.40 ft (42.7 cm)
Center of rotation, percent of duct chord	55.1	55.1
Center of rotation, fuselage station	22.50	62.82
Chord	0.73 ft (22.2 cm)	0.73 ft (22.2 cm)
Ratio of planform area to reference area	0.14	0.14
Duct chord plus exposed elevon chord	1.05 ft (32.0 cm)	1.21 ft (36.9 cm)

TABLE II.- COMPARISON OF AVERAGE MASS CHARACTERISTICS OF
MODEL (SCALED-UP) AND FULL-SCALE AIRPLANE

Characteristics	Model (scaled-up)		Full-scale airplane	
	U.S. Customary Unit	SI Unit	U.S. Customary Unit	SI Unit
Gross weight . .	14 360 lb	63 876 N	14 364 lb	63 893 N
Empty	------------	-----------	10 168 lb	45 229 N
I_X	24 700 slug-ft^2	33 450 kg-m^2	14 900 slug-ft^2	20 200 kg-m^2
I_Y	46 200 slug-ft^2	62 600 kg-m^2	33 605 slug-ft^2	45 600 kg-m^2
I_Z	61 400 slug-ft^2	83 200 kg-m^2	44 900 slug-ft^2	60 800 kg-m^2
w/S	63.81 lb/ft^2	3060 N/m^2	63.80 lb/ft^2	3060 N/m^2

TABLE III.- SCALING FACTORS

$$\begin{bmatrix} \text{Model (M) values to full-scale (FS) values.} \\ \text{(See ref. 1.)} \quad \text{Model scale} = 0.18 \text{ or } \dfrac{1}{5.56} \end{bmatrix}$$

$$\text{Length}_M \qquad \times 5.56 \qquad = \text{Length}_{FS}$$

$$\text{Weight}_M \qquad \times (5.56)^3 \qquad = \text{Weight}_{FS}$$

$$\text{Area}_M \qquad \times (5.56)^2 \qquad = \text{Area}_{FS}$$

$$\text{Inertia}_M \qquad \times (5.56)^5 \qquad = \text{Inertia}_{FS}$$

$$\text{Linear velocity}_M \quad \times (5.56)^{1/2} = \text{Linear velocity}_{FS}$$

$$\text{Angular velocity}_M \times \dfrac{1}{(5.56)^{1/2}} = \text{Angular velocity}_{FS}$$

L-63-10041

(a) Duct incidence angle set for hovering flight.

Figure 1.- Photographs of model.
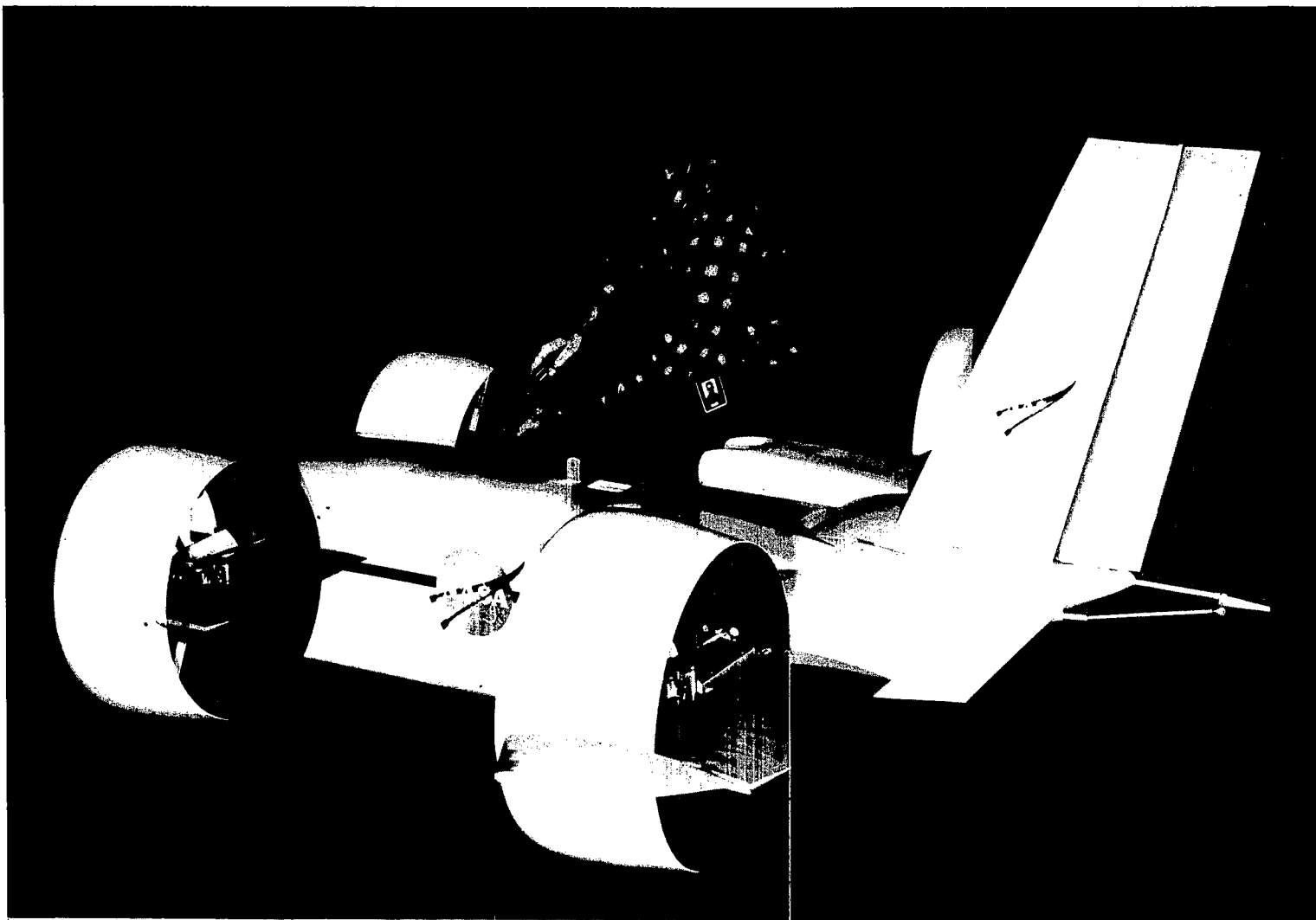
(b) Duct incidence angle set for cruising flight.

L-63-10044

Figure 1.- Concluded.
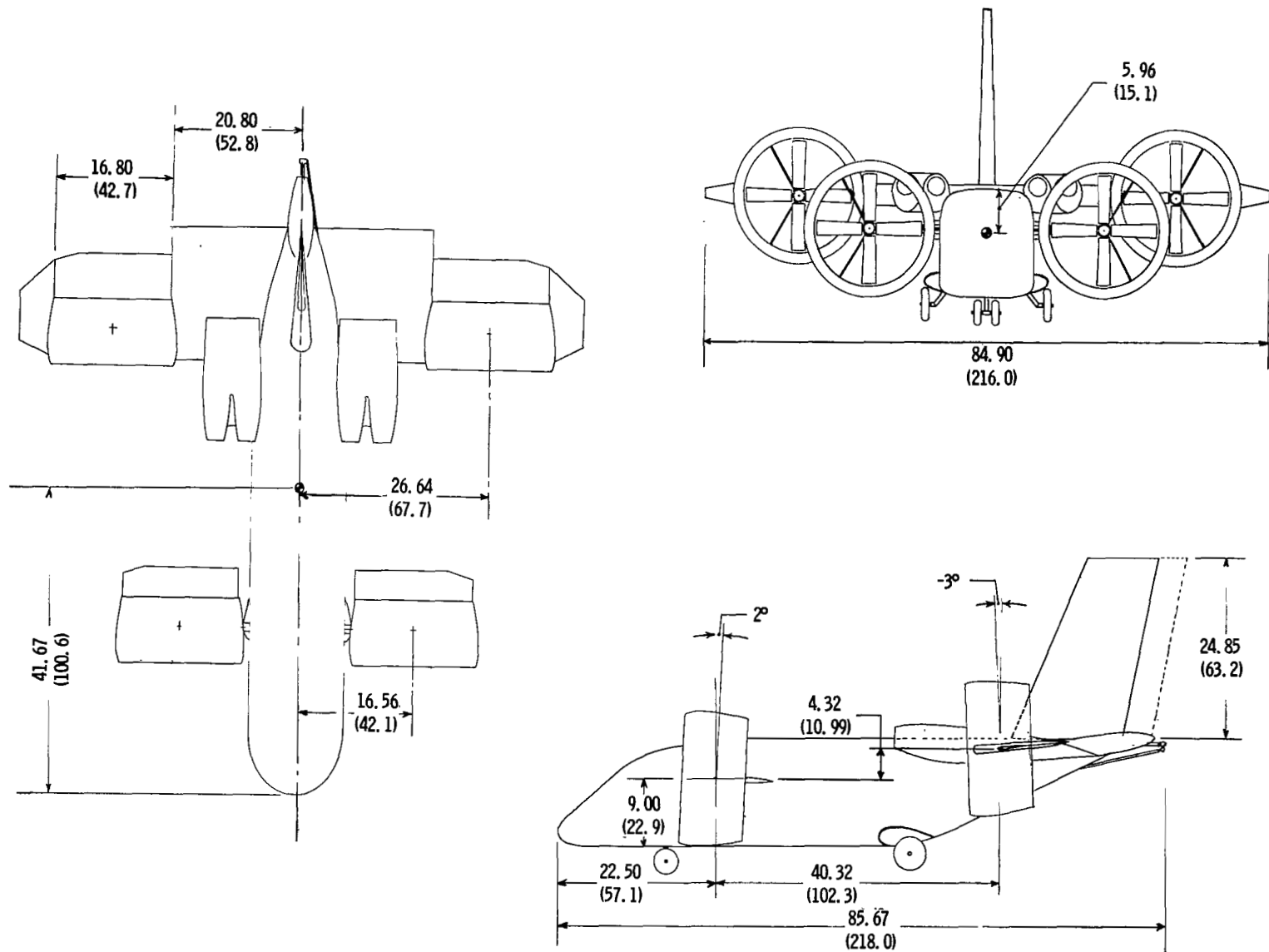
Figure 2.- Three-view sketch of model.   Dimensions are given first in inches and parenthetically in centimeters.
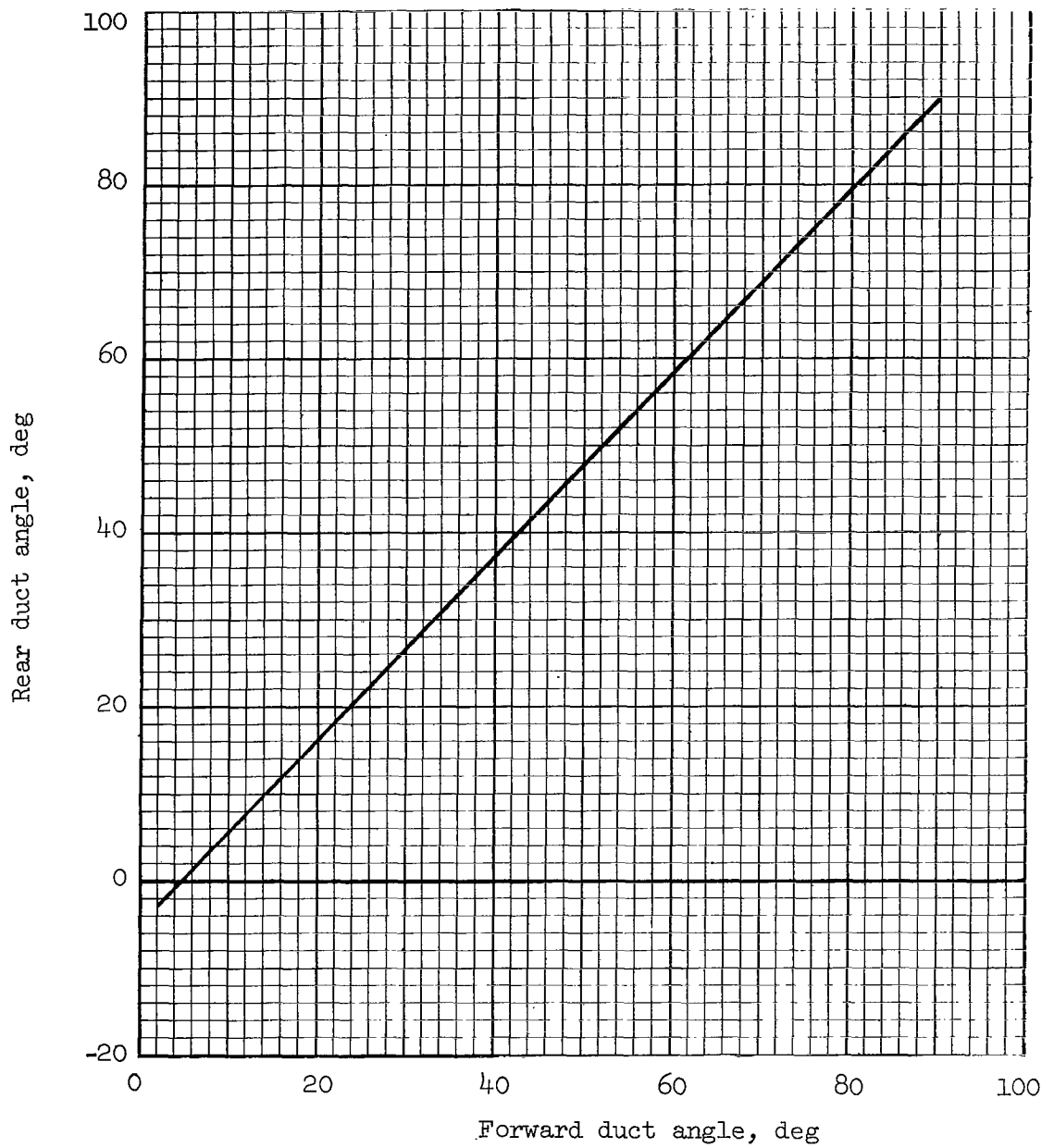
Figure 3.-   Programed relationship between forward-duct angle and rear-duct angle.

(a) Photograph of duct with fairing.

L-65-4030

Figure 4.- Details of antistall fairing installed on model duct.

8.82
(22.40)

A = Maximum lip thickness
B = Gradual thinning to zero
C = Zero lip thickness

C   C

B   B

30° ◄► 30°

A
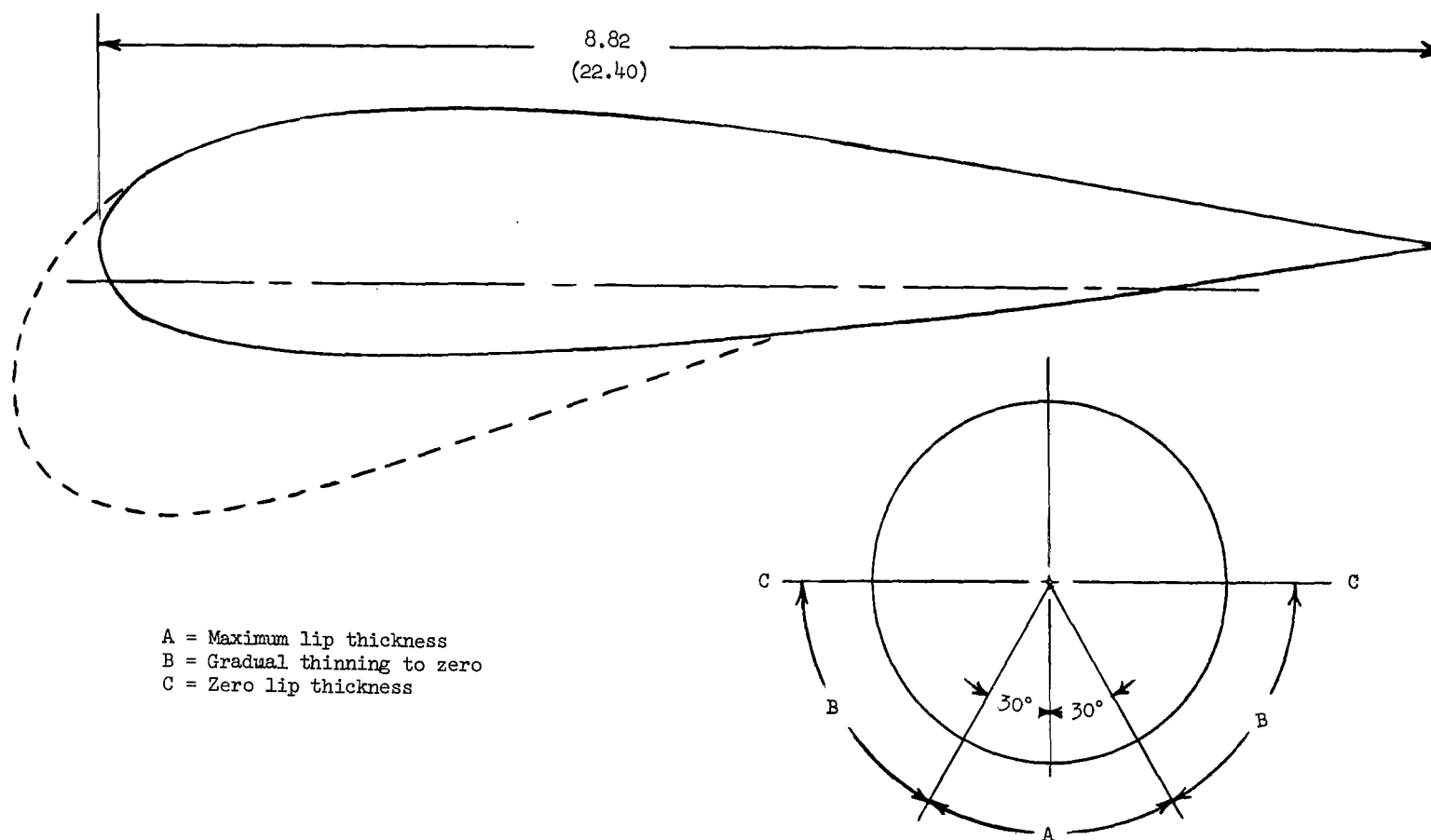
(b) Sketch of duct cross section showing position of lip fairing.

Figure 4.- Concluded.
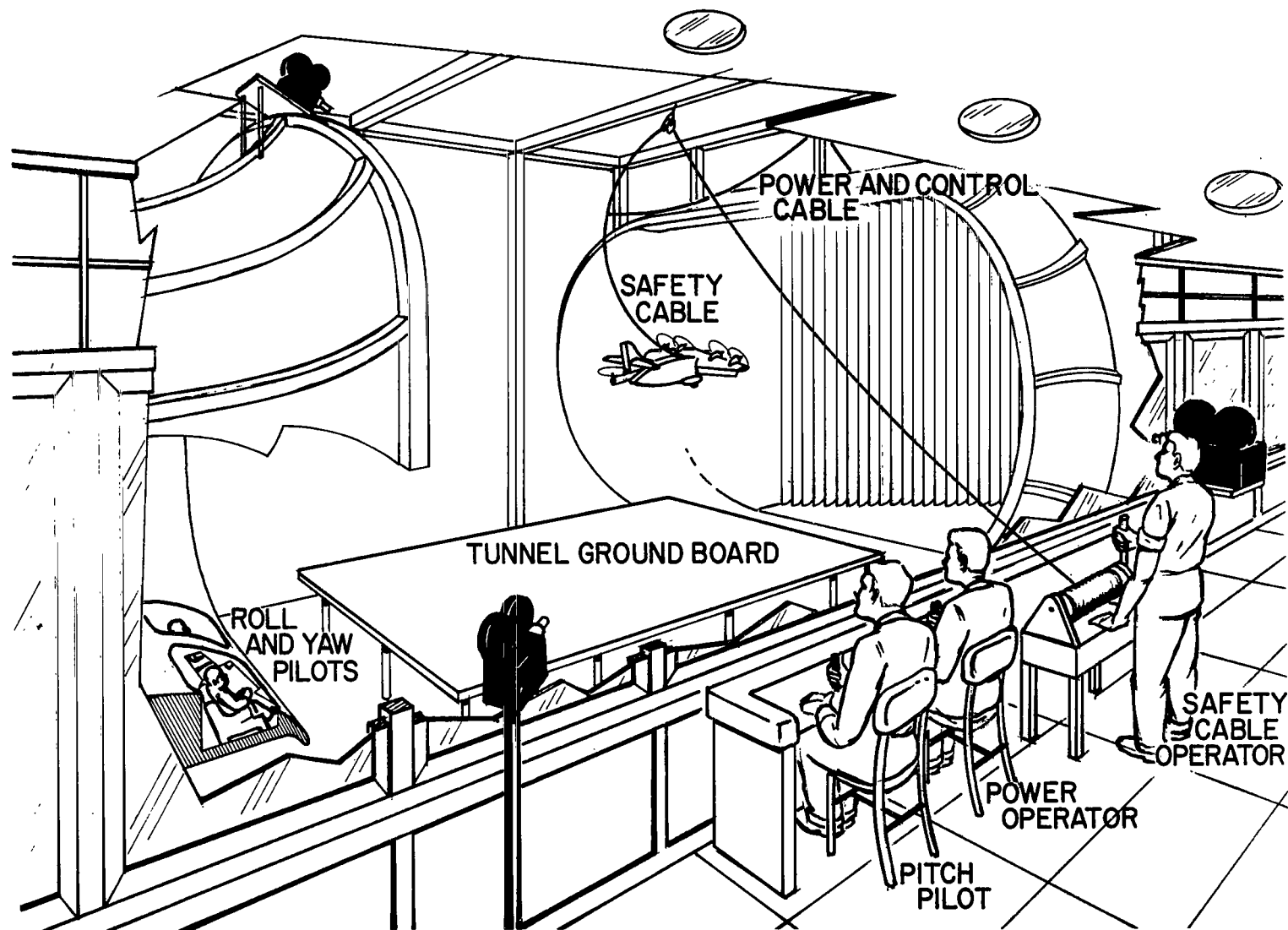
Figure 5.- Sketch of setup used for flight tests in the Langley full-scale tunnel.

L-64-3008
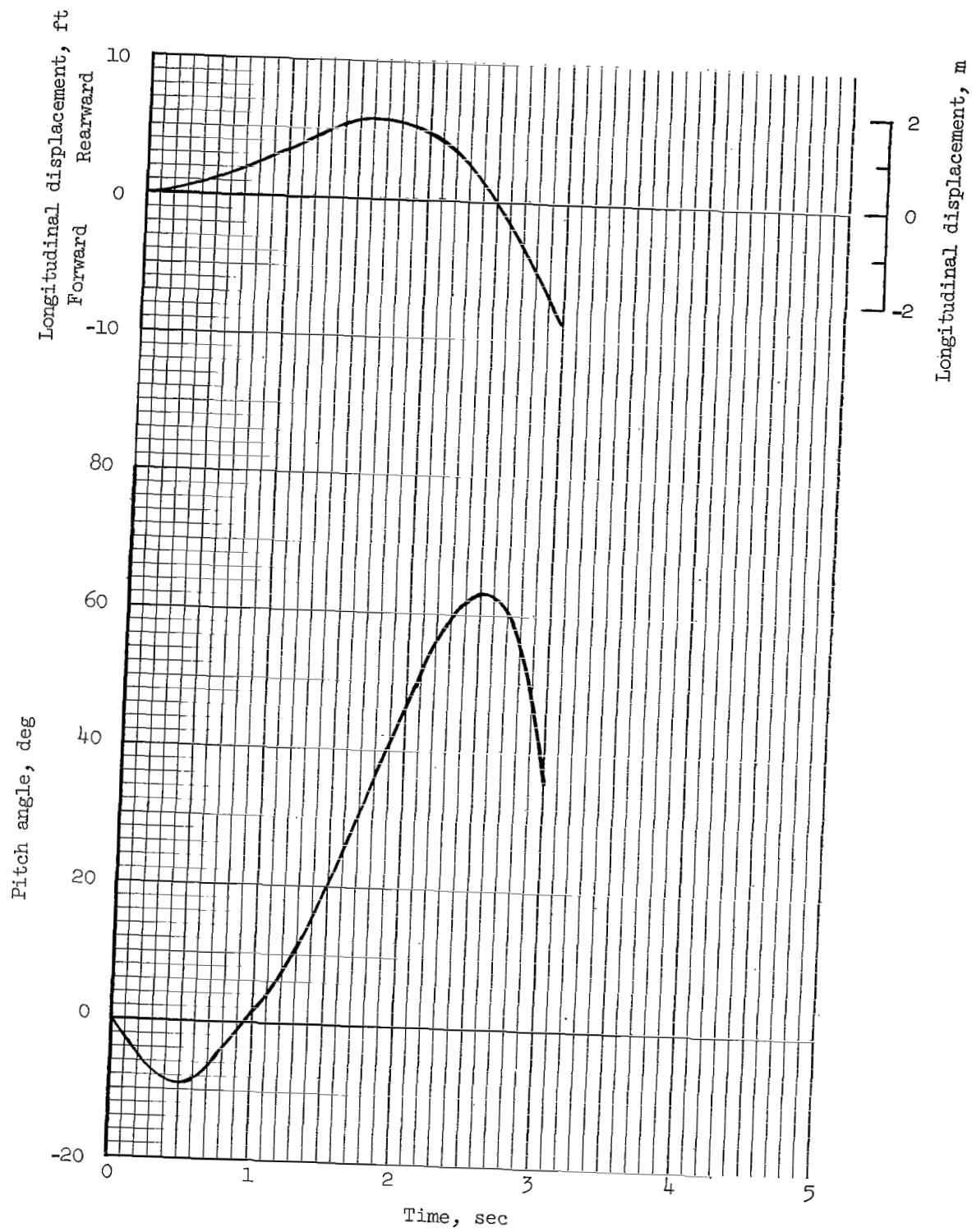
Figure 6.- Control-fixed pitching oscillation of model in hovering flight out of ground effect.

28
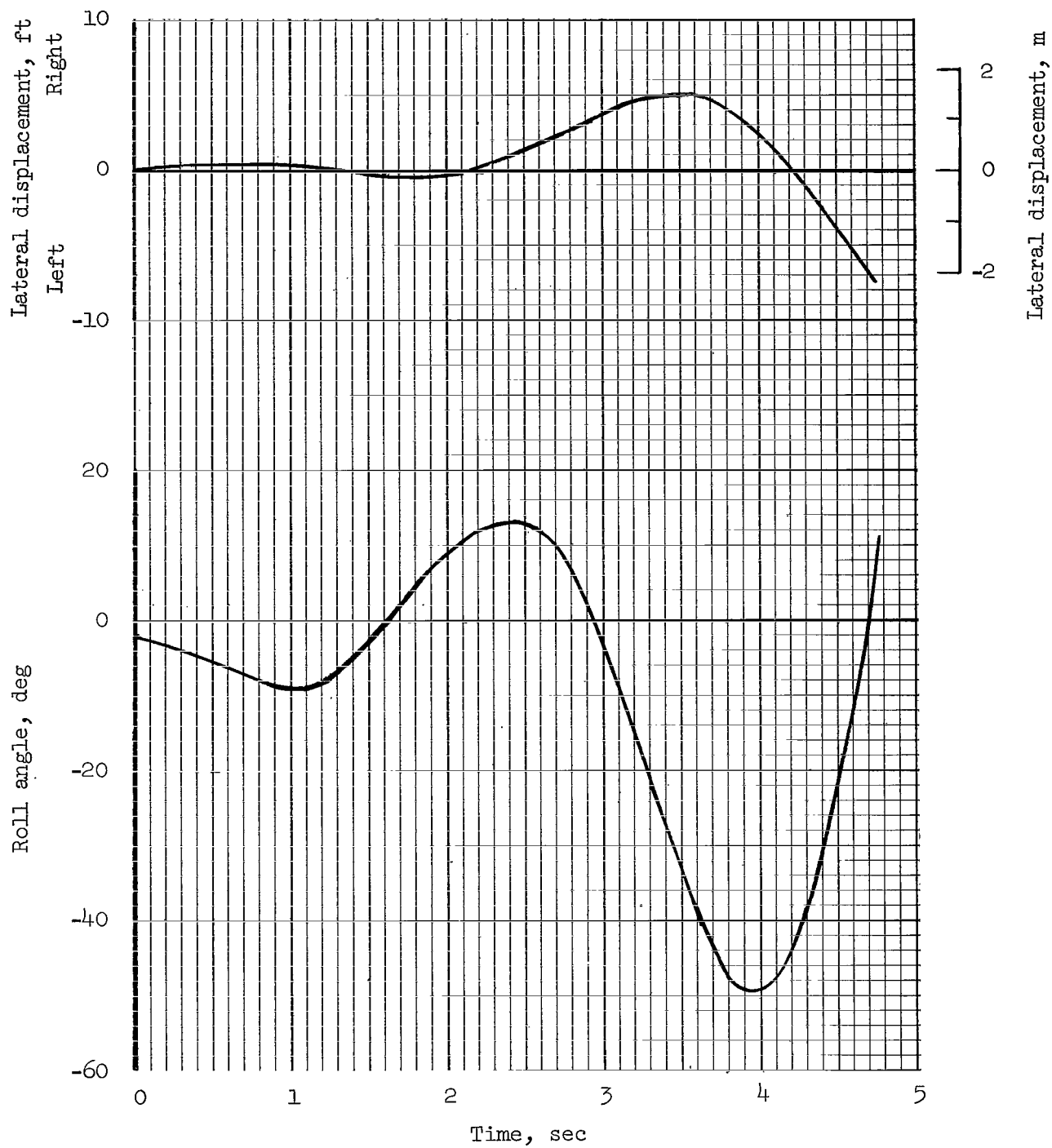
Figure 7.- Control-fixed rolling oscillation of model in hovering flight out of ground effect.
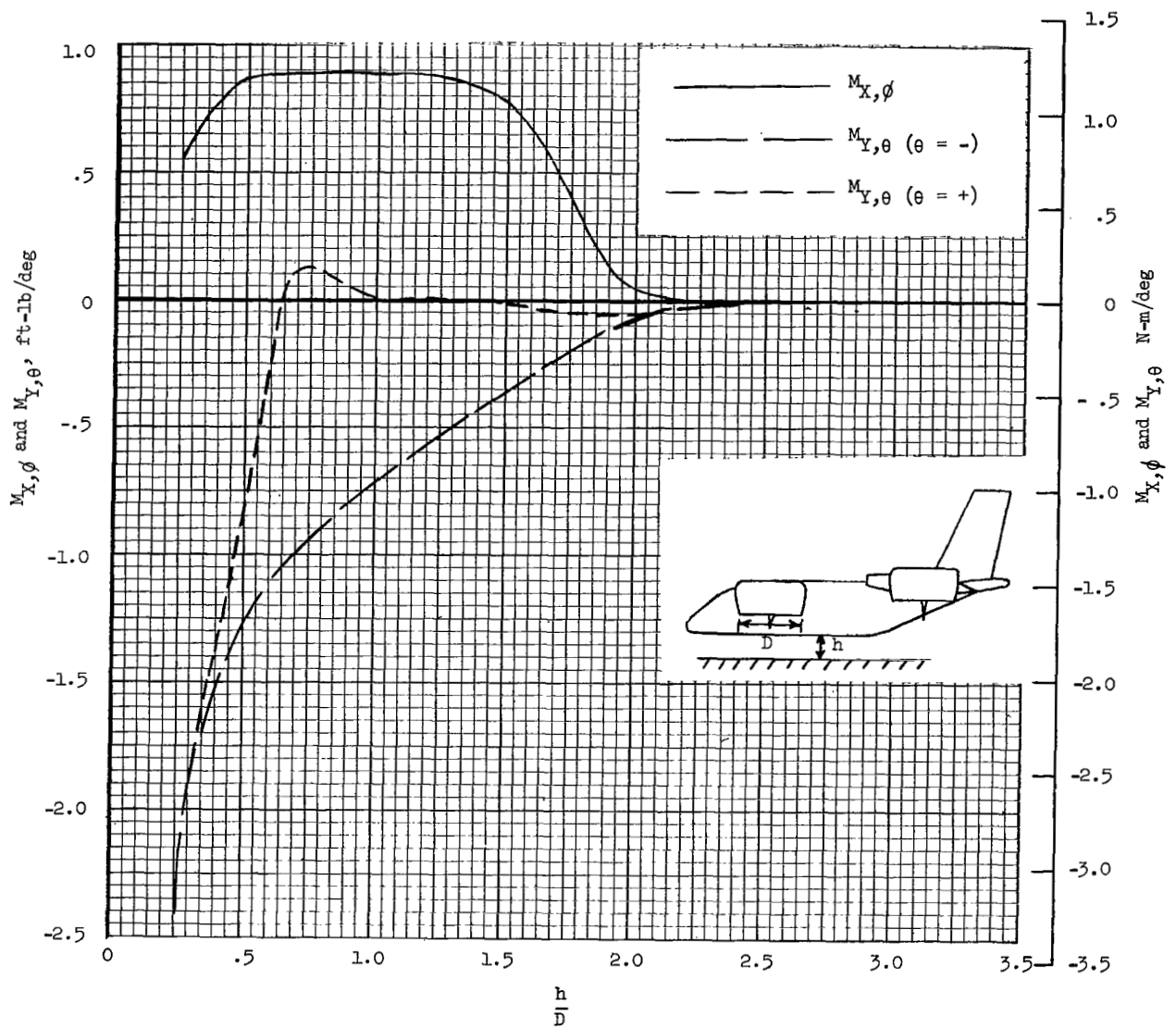
Figure 8.- Effect of ground proximity on static stability. Wheels touch at $\frac{h}{D} \approx 0.28$.
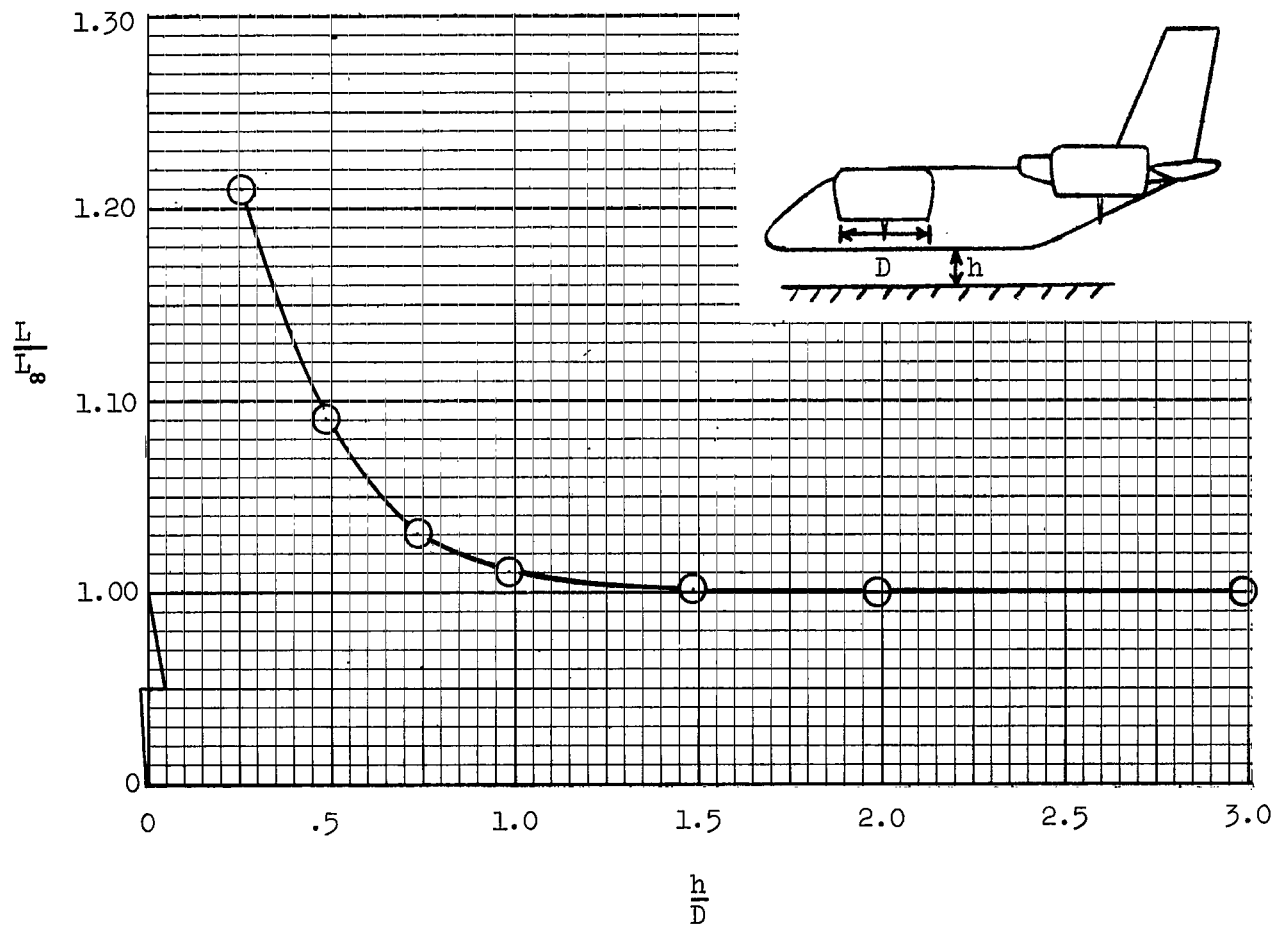
Figure 9.- Effect of ground proximity on lift at constant propeller rotational speed and blade pitch angle. Wheels touch at $\frac{h}{D} \approx 0.28$.
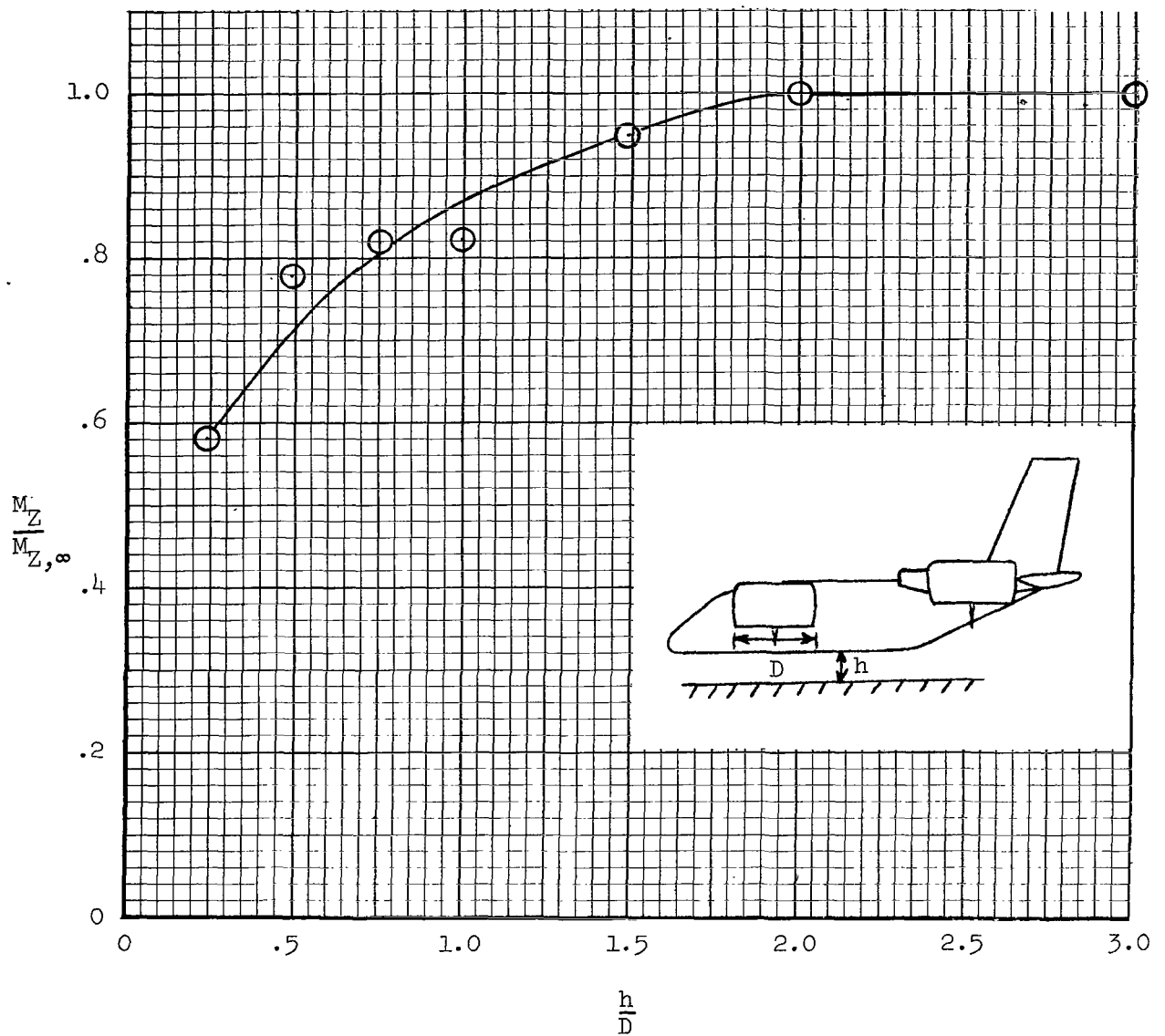
Figure 10.- Effect of ground proximity on aileron yaw-control effectiveness. Wheels touch at $\frac{h}{D} \approx 0.28$. $\delta_e = \pm 24^0$.
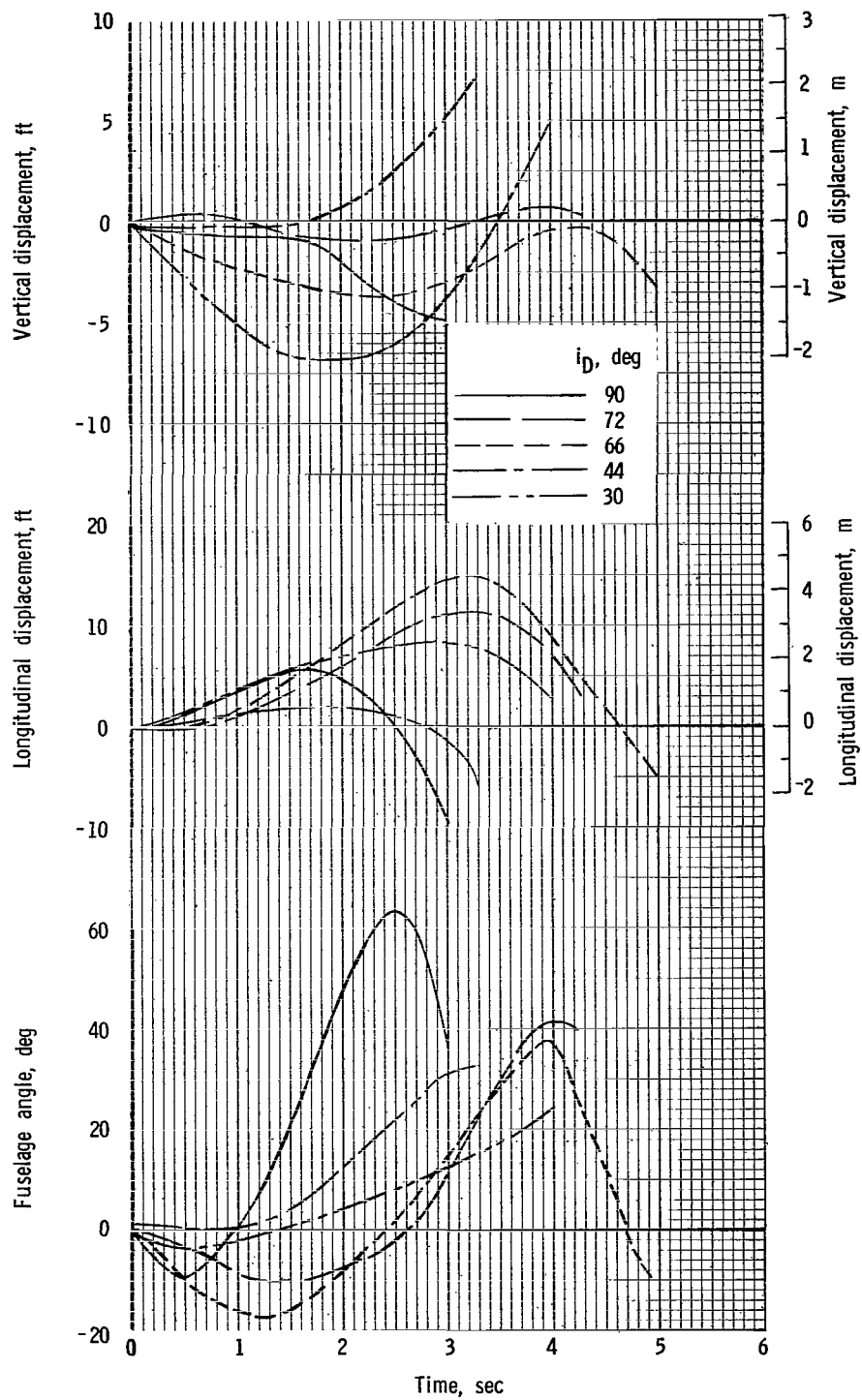
Figure 11.- Control-fixed longitudinal motions of model in transition flight range.
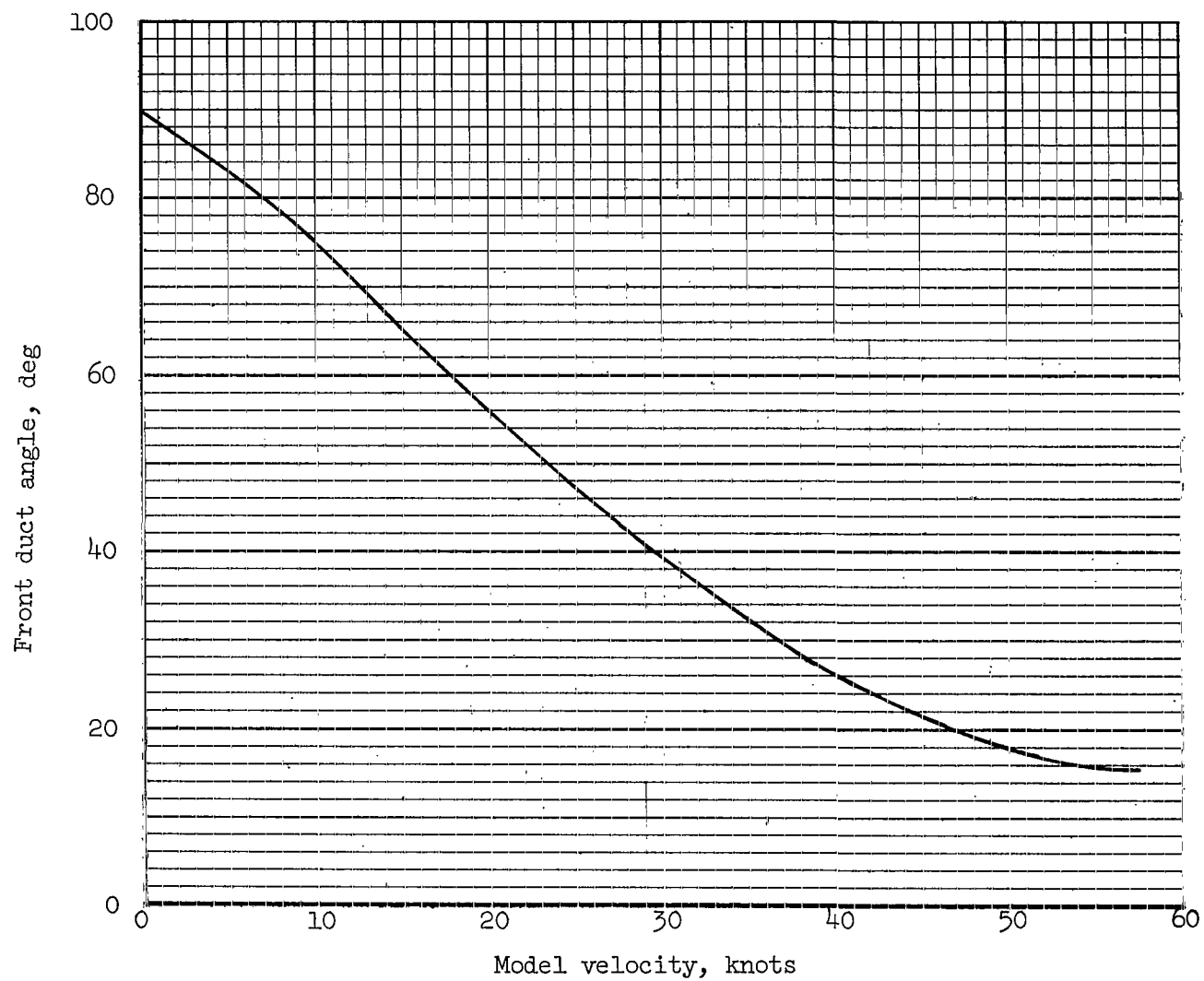
Figure 12.- Variation of model velocity with front-duct incidence angle. Fuselage angle, $\alpha = 0^0$.
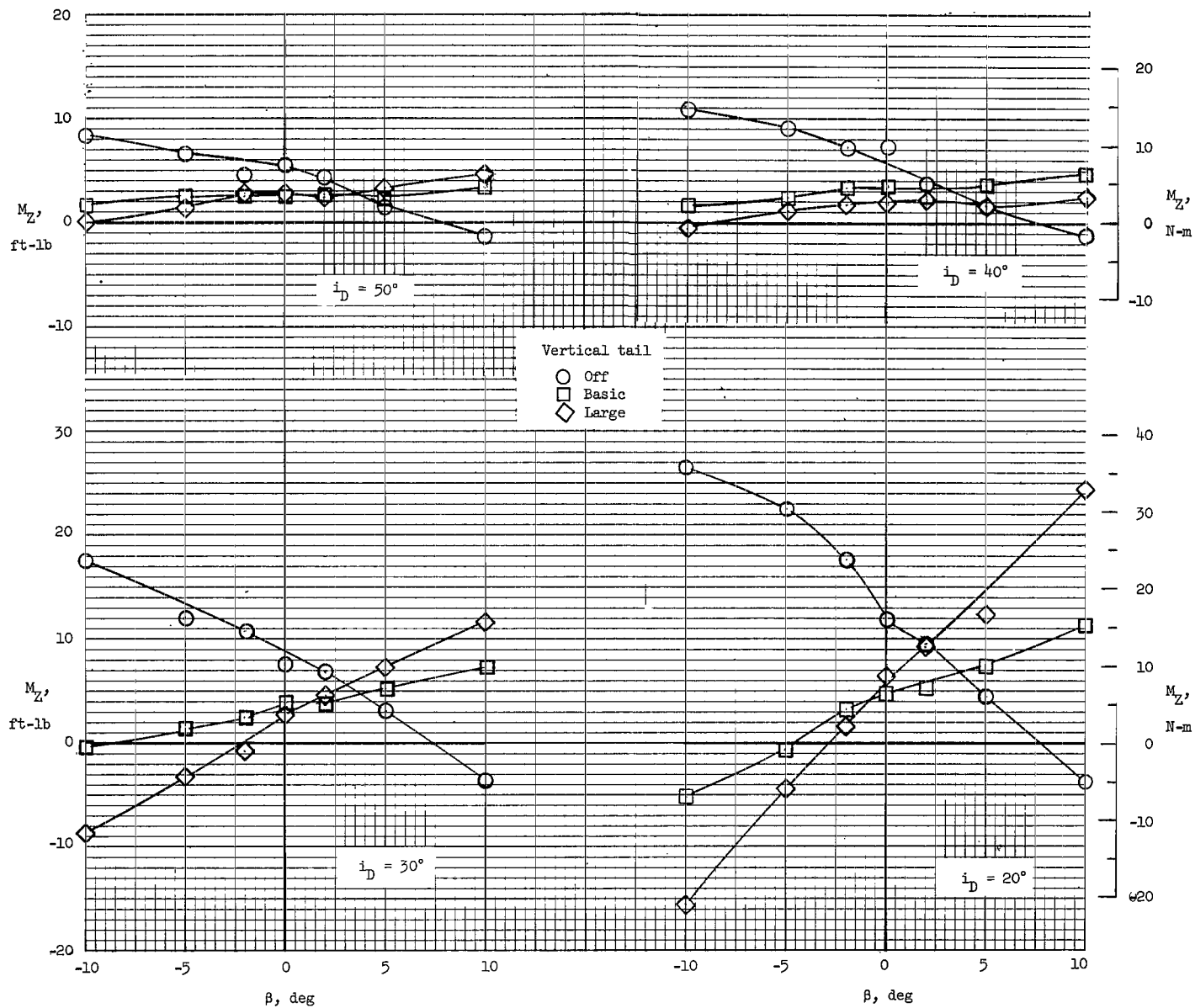
Figure 13.- Effect of vertical-tail size on variation of yawing moment with sideslip in transition flight range. α = 0⁰; drag = 0.

(a) $\alpha = -1^0$.
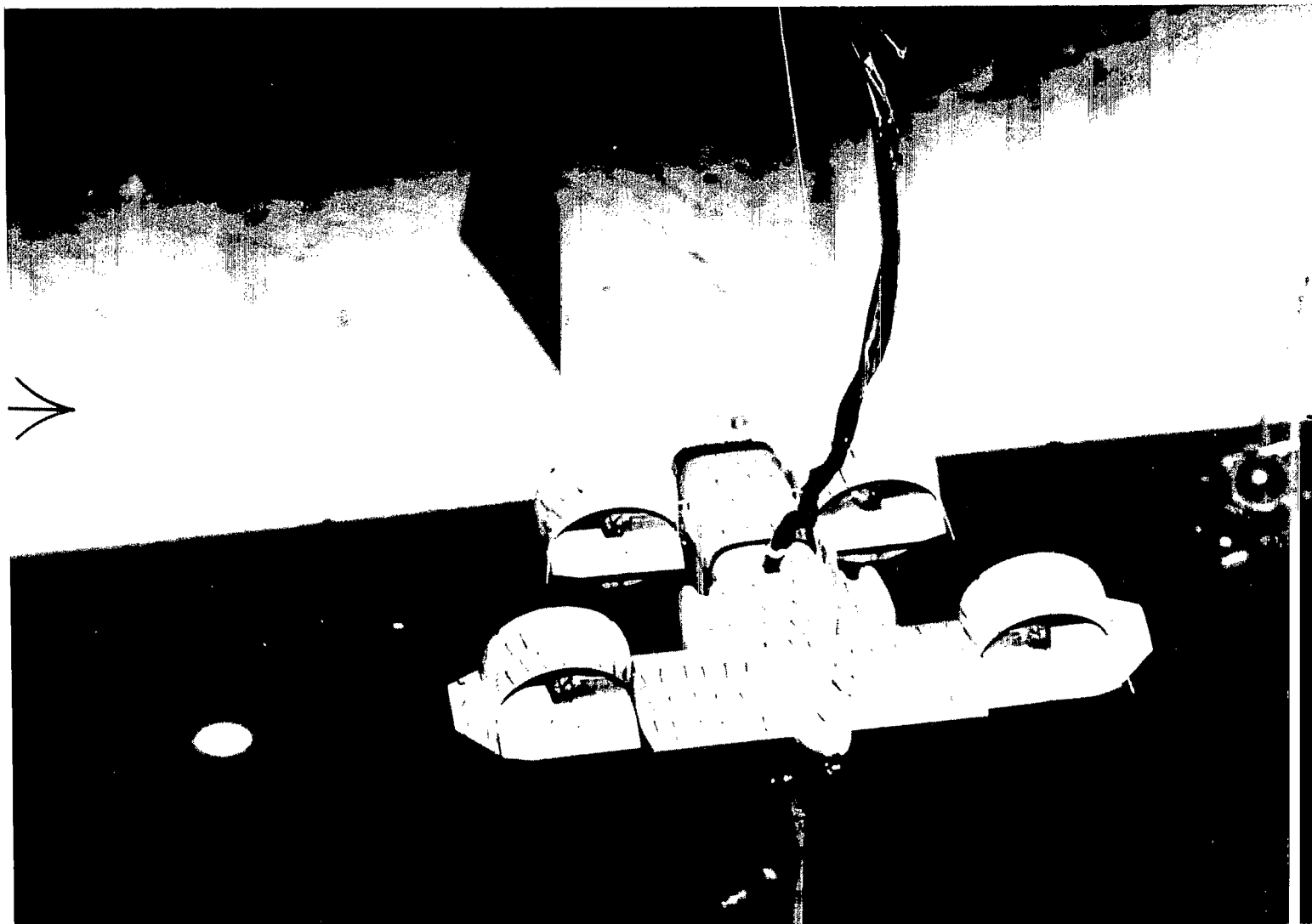
L-65-7907

Figure 14.- Photographs of a typical series of tuft tests showing variation of duct upper-surface stall with angle of attack. $i_D = 20^0$.

(b) $\alpha = 1^0$.

Figure 14.- Continued.

(c) $\alpha = 2^0$.
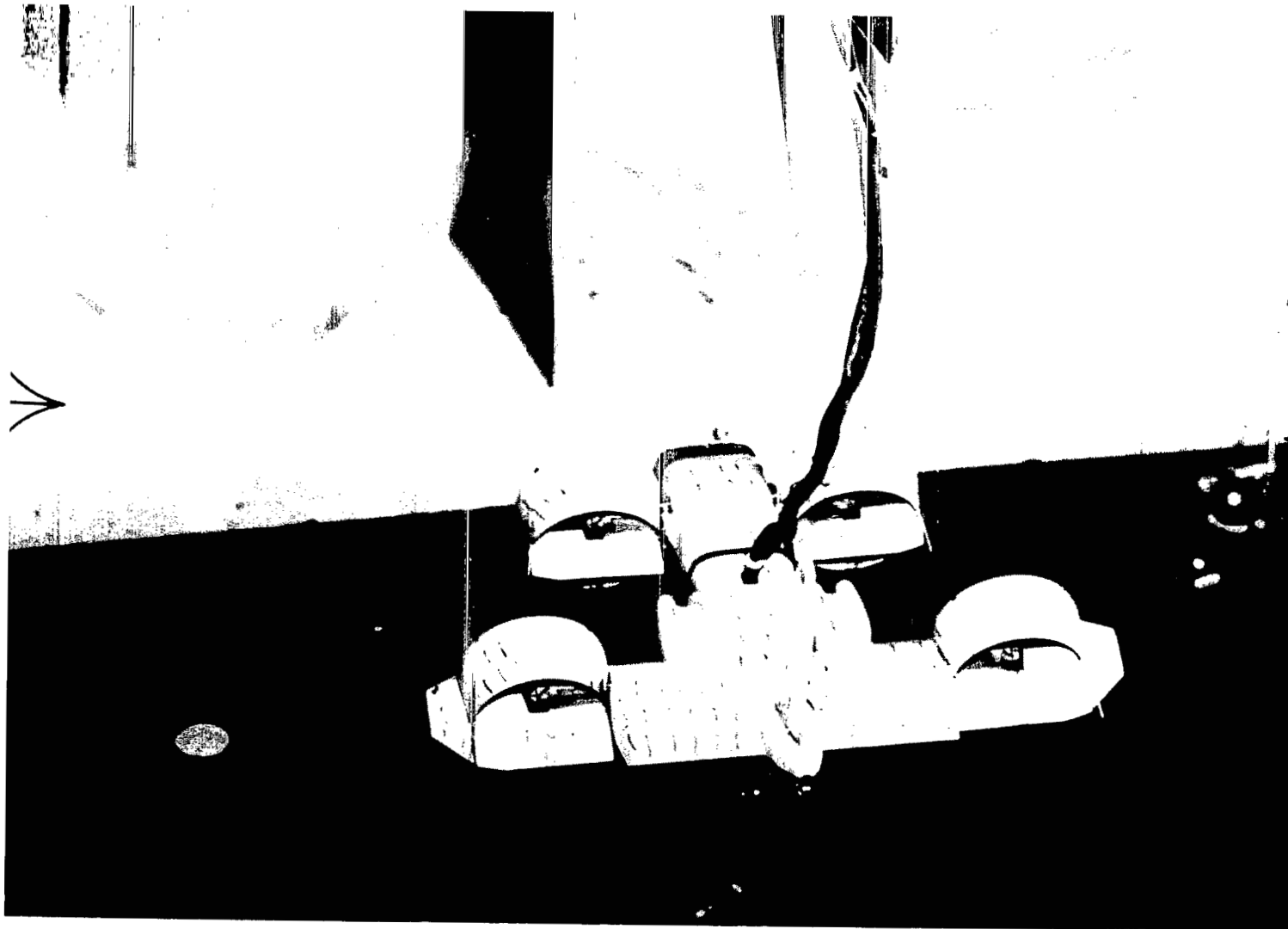
Figure 14.- Continued.

L-65-7909

(d) $\alpha = 5^0$.

Figure 14.- Continued.

(e) $\alpha = 6^0$.

L-65-7911

Figure 14.- Concluded.

.20 Diam.
(.51)

.1
(.25)

.3
(.76)

.3
(.76)

.9
(2.29)

.3
(.76)

.43
(1.09)

.75
(1.91)

.75
(1.91)

.75
(1.91)

22.5°

.75
(1.91)

22.5°

.44
(1.12)

.05 c_D
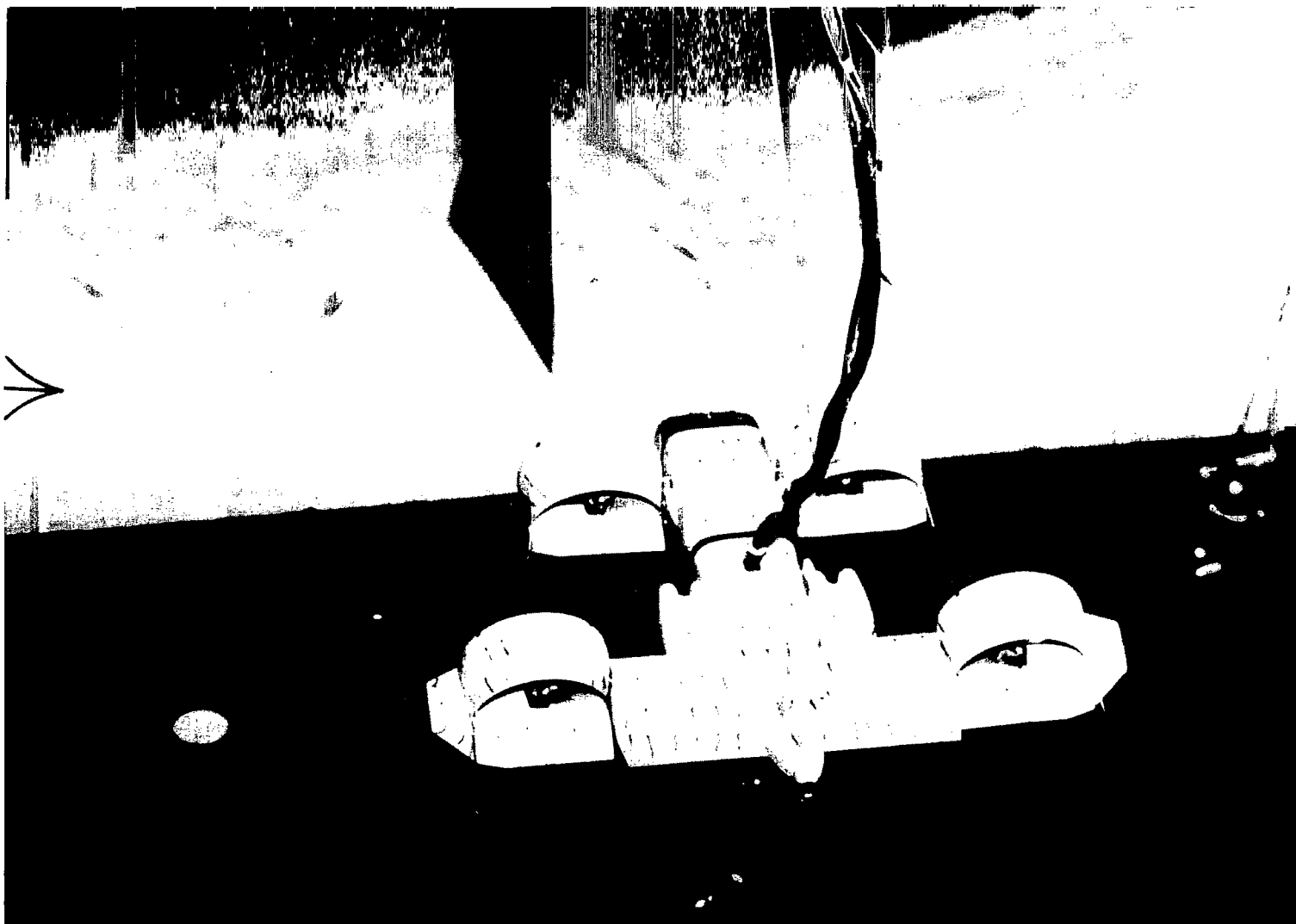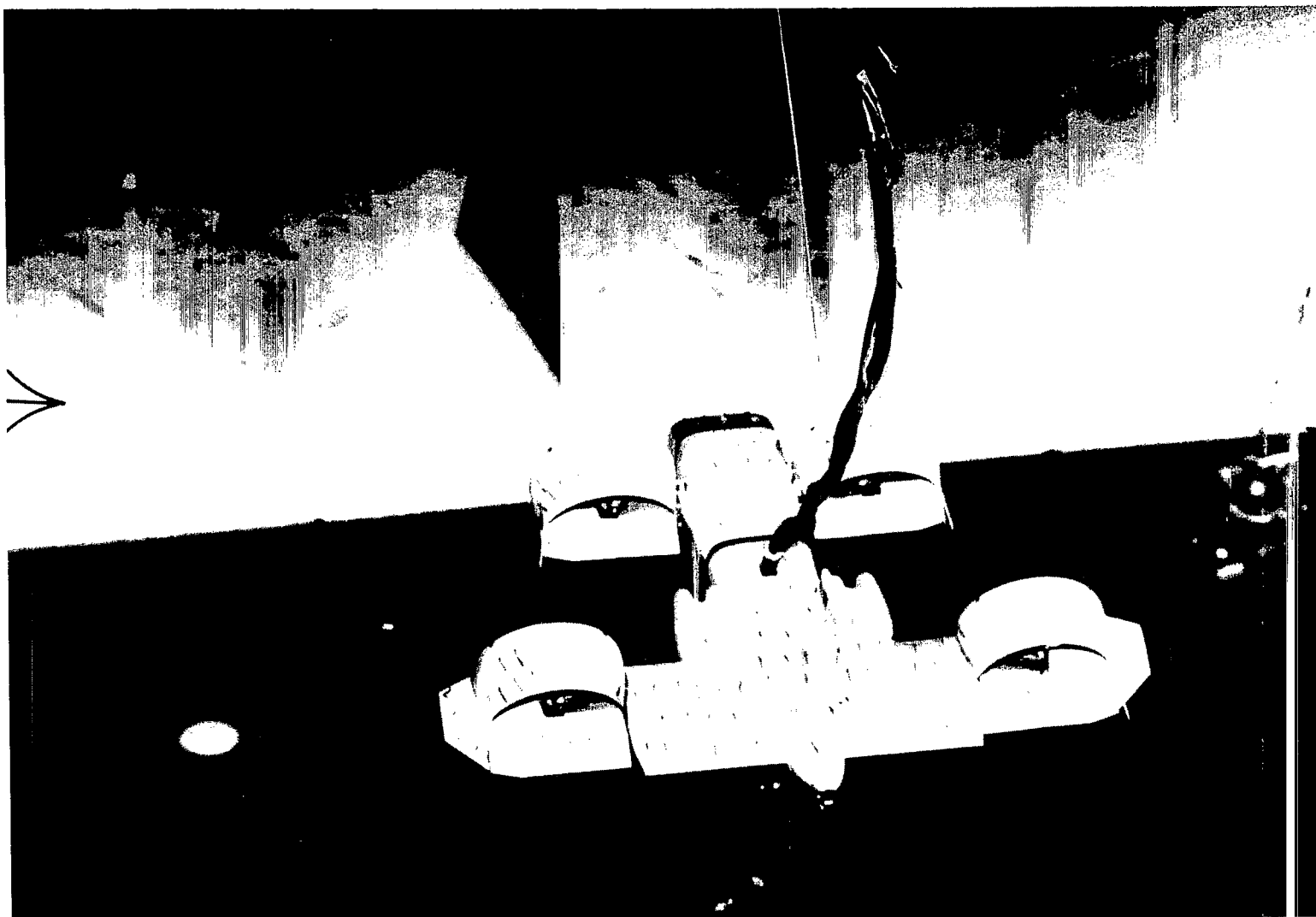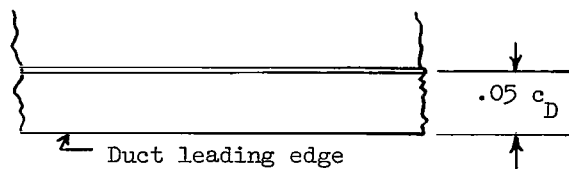
Trip Wire
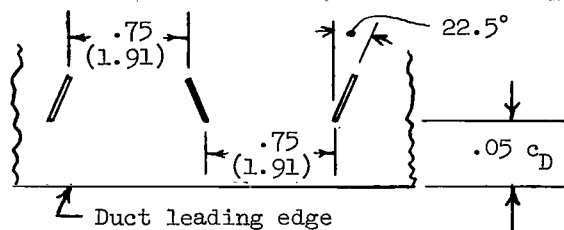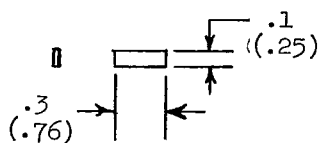
Small Vanes
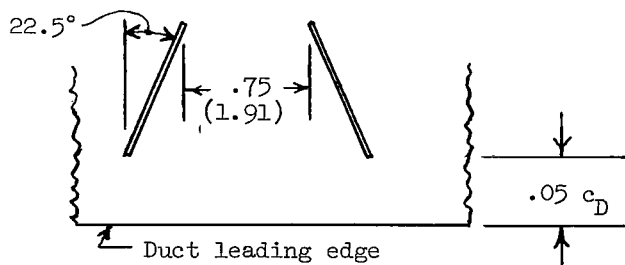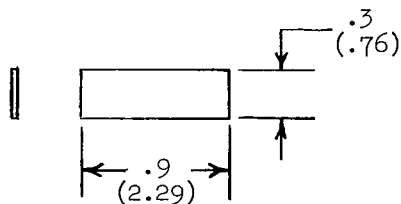
Large Vanes
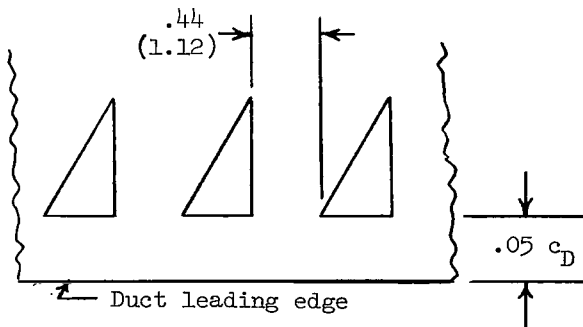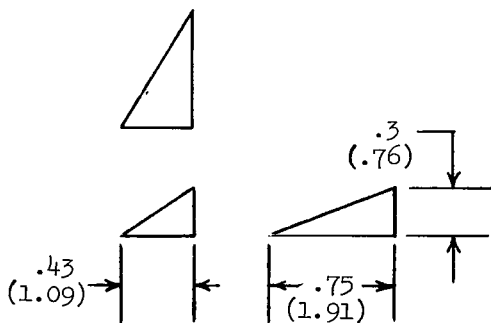
Wedges

Figure 15.- Four types of vortex generators used on duct upper surface. Upper dimensional number in inches. Lower dimensional number in centimeters.

Cross-section at top center line

Cross-section at pivot

.3
(.76)

15°

.1
(.25)

.7
(1.77)

1.1
(2.79)

8.82
(22.40)
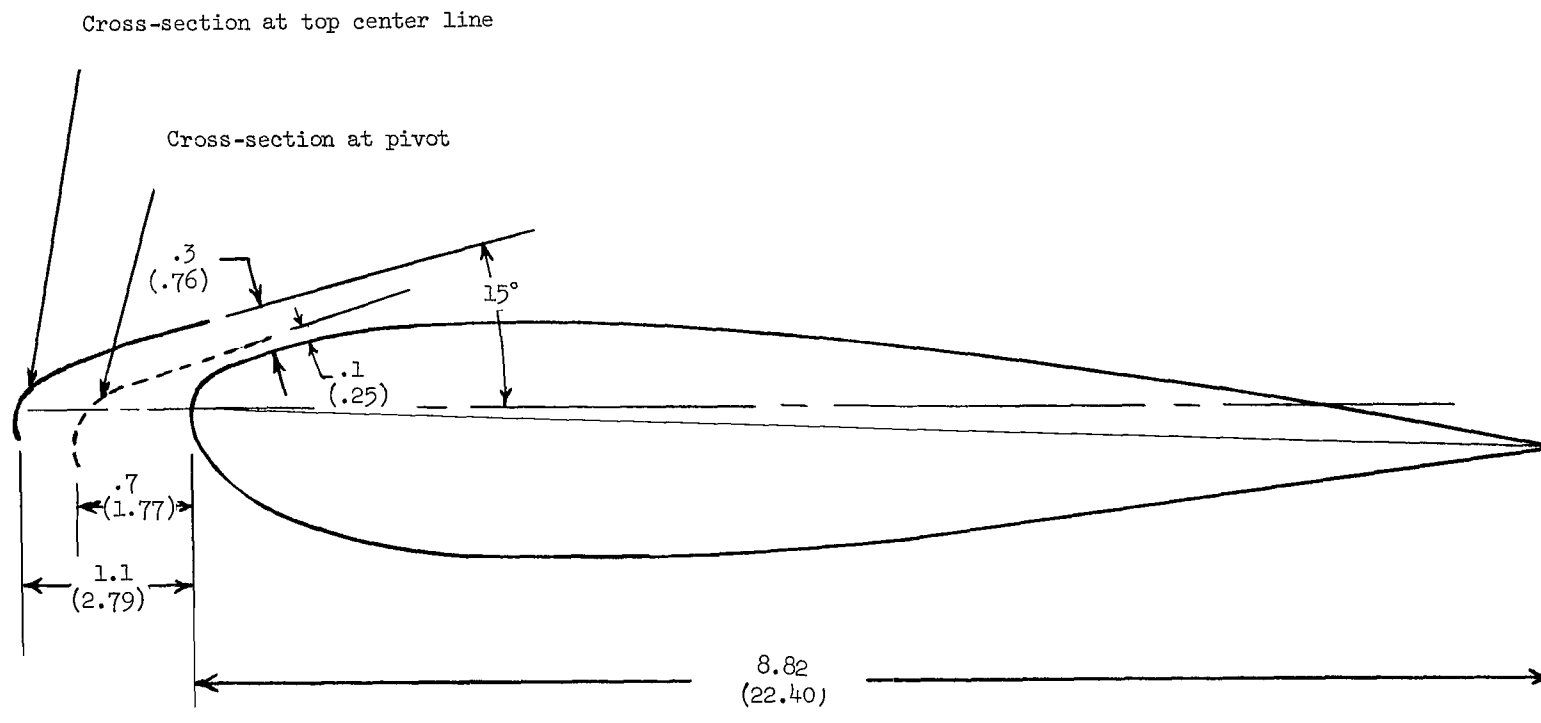
(a) Sketch of duct showing cross sections with slat in position.

Figure 16.- Details of model ducts. Dimensions are given first in inches and parenthetically in centimeters.
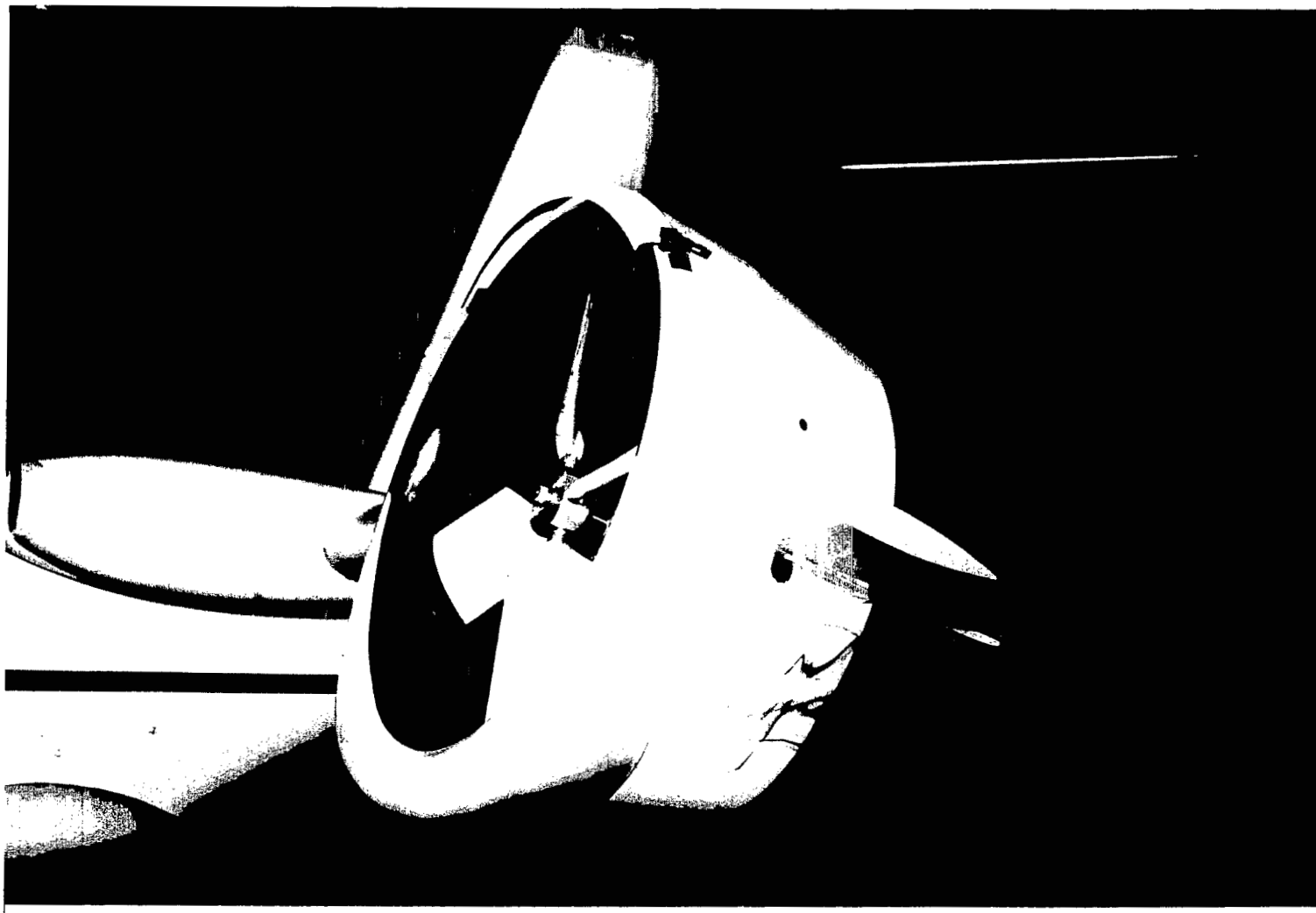
(b) Photograph of duct showing slat mounted at top and large-radius fairing mounted at bottom leading edges.
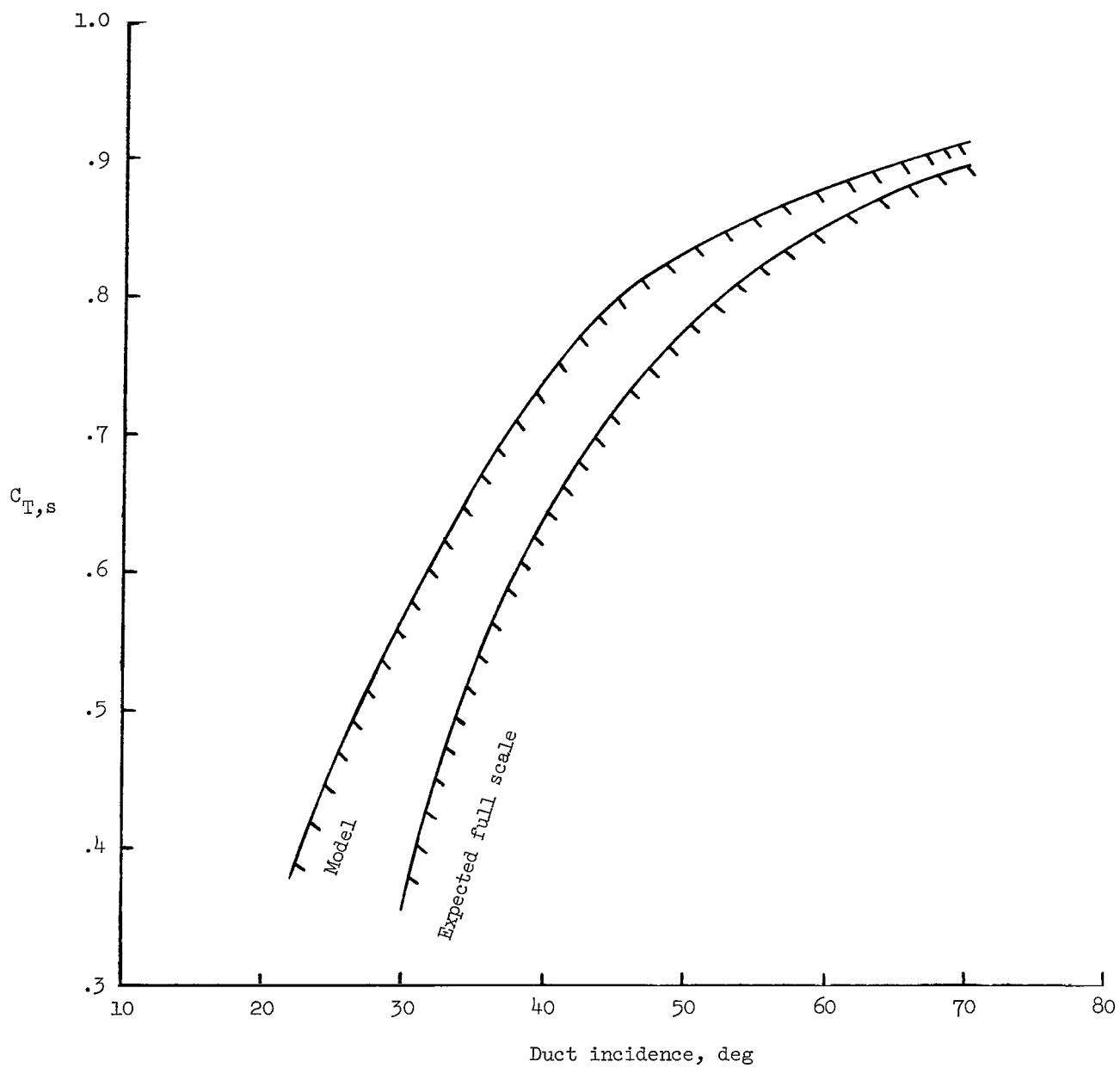
Figure 16.- Concluded.

L-65-3703

Figure 17.- Comparison of duct upper-surface stall boundaries for 0.18-scale model and full-scale airplane. $\alpha = 0^0$.
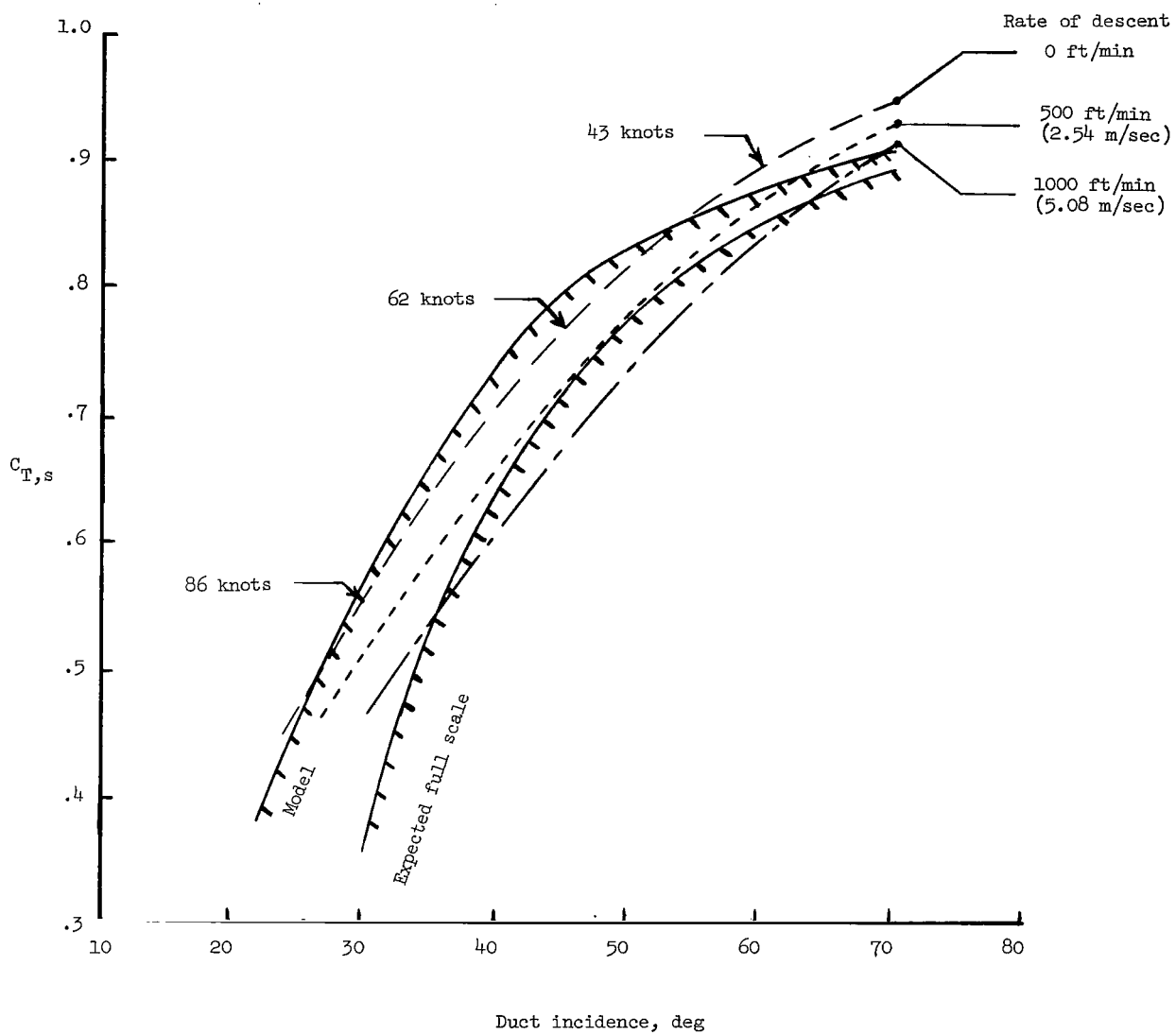
Figure 18.- Model and full-scale stall boundaries related to various descent rates. Data from figure 17. $\alpha = 0^0$.
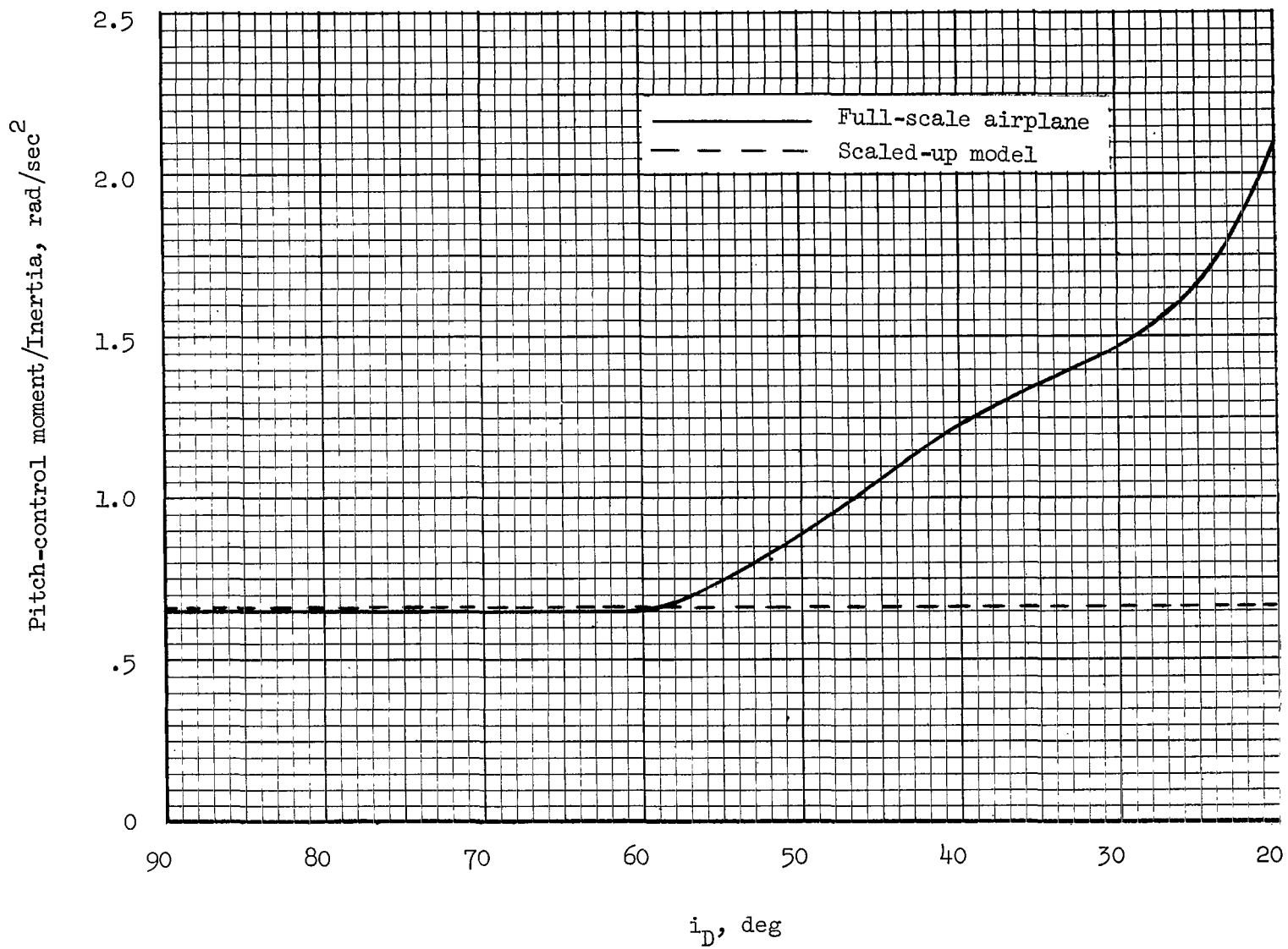
Figure 19.- Longitudinal control power available in excess of that required for trim on the full-scale airplane compared with scaled-up model control power required in tests.
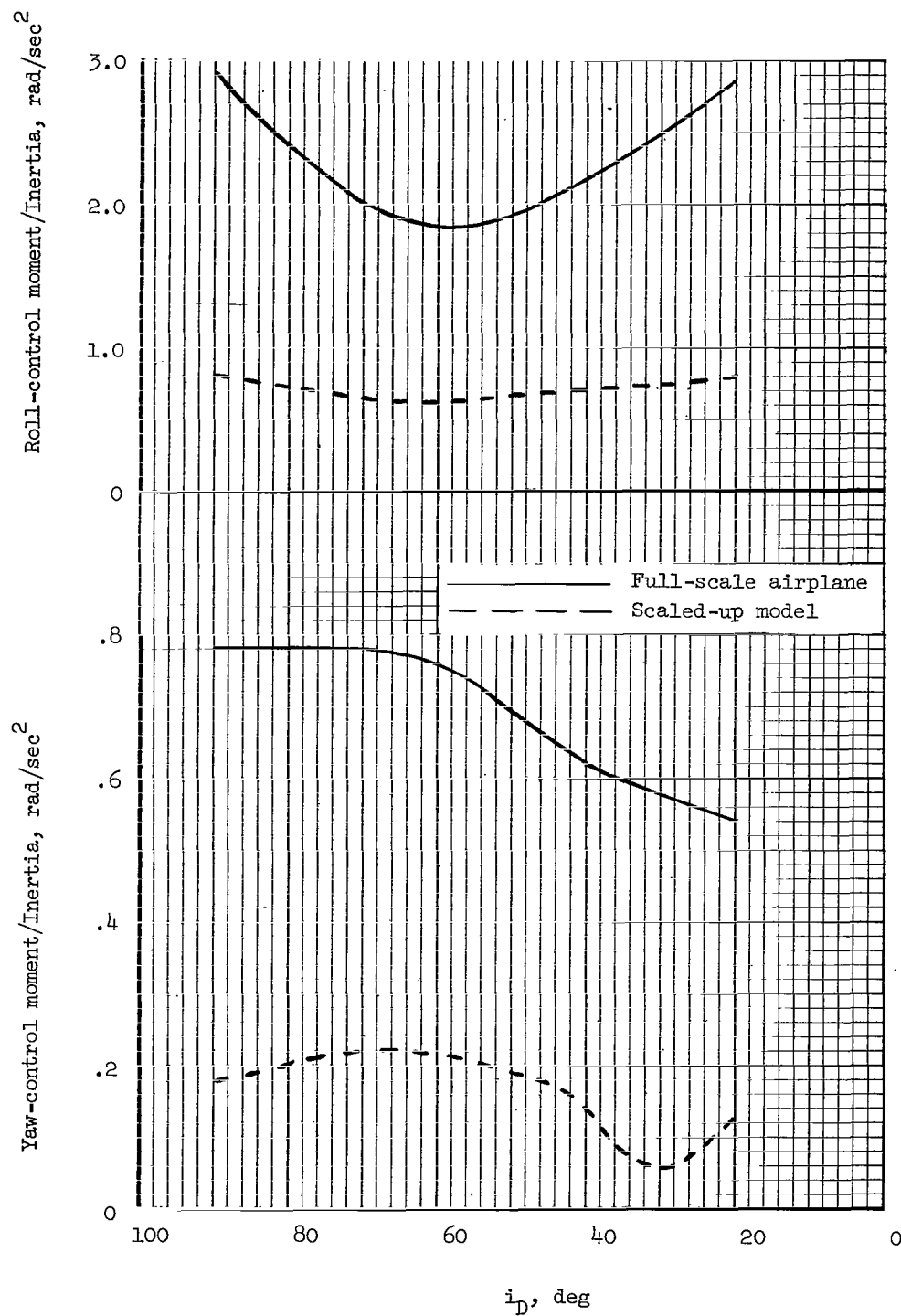
Figure 20.- Lateral control power available on airplane compared with scaled-up model control power required in tests.

"The aeronautical and space activities of the United States shall be conducted so as to contribute . . . to the expansion of human knowledge of phenomena in the atmosphere and space. The Administration shall provide for the widest practicable and appropriate dissemination of information concerning its activities and the results thereof."

—NATIONAL AERONAUTICS AND SPACE ACT OF 1958

NASA SCIENTIFIC AND TECHNICAL PUBLICATIONS

TECHNICAL REPORTS: Scientific and technical information considered important, complete, and a lasting contribution to existing knowledge.

TECHNICAL NOTES: Information less broad in scope but nevertheless of importance as a contribution to existing knowledge.

TECHNICAL MEMORANDUMS: Information receiving limited distribution because of preliminary data, security classification, or other reasons.

CONTRACTOR REPORTS: Technical information generated in connection with a NASA contract or grant and released under NASA auspices.

TECHNICAL TRANSLATIONS: Information published in a foreign language considered to merit NASA distribution in English.

TECHNICAL REPRINTS: Information derived from NASA activities and initially published in the form of journal articles.

SPECIAL PUBLICATIONS: Information derived from or of value to NASA activities but not necessarily reporting the results of individual NASA-programmed scientific efforts. Publications include conference proceedings, monographs, data compilations, handbooks, sourcebooks, and special bibliographies.

Details on the availability of these publications may be obtained from:

SCIENTIFIC AND TECHNICAL INFORMATION DIVISION

NATIONAL AERONAUTICS AND SPACE ADMINISTRATION

Washington, D.C. 20546